CHEMICAL REVIEWS

Review

Organocuprates and Diamagnetic Copper Complexes: Structures and NMR Spectroscopic Structure Elucidation in Solution

Ruth M. Gschwind

Chem. Rev., **2008**, 108 (8), 3029-3053 • DOI: 10.1021/cr800286r • Publication Date (Web): 13 August 2008

Organocuprates and Diamagnetic Copper Complexes: Structures and NMR Spectroscopic Structure Elucidation in Solution

Ruth M. Gschwind*

Institut für Organische Chemie, Universität Regensburg, Universitätsstrasse 31, D-93040 Regensburg, Germany

Received April 11, 2008

Contents

1. Introduction

A key role of copper is generally accepted in various scientific fields, for example, in organic synthesis for the formation of C−C bonds, in superconductors, and in biological oxygenation processes. The structure elucidation of copper complexes in solution and the characterization of the electronic structure and bonding at Cu sites greatly benefit chemists and structural biologists in systems such as organometallic copper compounds (for selected articles and reviews see refs 1–8), copper proteins,[9–12] amyloid related peptides,[13] or copper model systems relevant to organocopper chemistry and biological systems.[14–17] This is because detailed structural information is often essential for understanding the mechanisms that afford the enormous synthetic and biological potential of Cu(I)/Cu(III) and Cu(I)/Cu(II) redox systems. In solution, the spectroscopic methods, applied in structure elucidation processes, differ substantially between Cu(I)/Cu(III) compounds and systems containing Cu(II). This is due to the different magnetic properties of Cu(II) compared to Cu(I) and square planar Cu(III) complexes. Because Cu(II) is paramagnetic, electron spin resonance (ESR) spectroscopy is mainly applied to the solution state structure determination of Cu(II) containing systems. On the other hand, high resolution NMR spectroscopy is the method of choice for diamagnetic Cu(I) and Cu(III) compounds. For large proteins, paramagnetic NMR spectroscopy forms the link between the two methods and has been performed with great success.[18,19] In protein structure elucidation, the marginal deviations between solid state and solution structures often allow a direct transfer of information from X-ray crystallographical data. In contrast, the radii of Cu(II) containing organometallic compounds and chiral copper complexes are usually so small that paramagnetic NMR is hardly feasible because of extreme line broadening effects. Therefore, the absence of Cu(II) is of great importance for the successful application of high resolution NMR spectroscopy of diamagnetic complexes as narrow line widths are indispensible. For example, in ^{63}Cu NMR spectroscopy, the broadenings of the copper signals are 2% when 1% of the copper is present as copper(II), whereas an increase in the copper(II) content to 9% results in a line broadening effect of 870%.[20] In addition, the solvent effects on the structures and reactivities of organocopper compounds are legendary. Therefore, for organocopper compounds in solution, the existence or dominance of a structure cannot be inferred directly from crystal structures and the solution aggregation numbers and aggregate sizes must be determined independently. Considering the different spectroscopic approaches for paramagnetic, diamagnetic, biomacromolecular, and organometallic systems, a comprehensive coverage of all these methods is far beyond the scope of this article. To address copper compounds, which are important for applications in organic synthesis, this review focuses on the NMR spectroscopic structure elucidation and the resulting structures of small diamagnetic Cu(I) and Cu(III) organocuprates and copper complexes in solution.

At first, the principles and the application range of $^{63/65}$Cu NMR in solution is described. Due to the large quadrupole moments of ^{63}Cu and ^{65}Cu, the scope of $^{63/65}$Cu NMR in solution is limited to some highly symmetric complexes with

* To whom correspondence should be addressed. E-mail: ruth.gschwind@chemie.uni-regensburg.de. Phone: ++49 +941 943 4625. Fax: ++49 +941 943 4617.

10.1021/cr800286r CCC: $71.00
Published on Web 08/13/2008

Ruth M. Gschwind received her Ph.D from the Technical University of Munich in 1997 under the supervision of Prof. H. Kessler. She started her habilitation (equivalent to Assistant Professorship) at the University of Marburg in 1997, joined the faculty at the University of Bonn as Associate Professor in 2002, and moved to the University of Regensburg in 2005. Her research interest is the structural and mechanistic understanding and optimization of organometallic and bioorganic supramolecular complexes using NMR spectroscopy as main method.

an undisturbed tetrahedral coordination of the copper ions. Despite this restriction, structural information can be obtained about the π-acceptor properties of ligands, the symmetry of the complexes, and ligand exchange processes.

However, most of the synthetically important copper complexes are less symmetrical and show lower coordination numbers on copper. This facilitates the formation of intermediate structures with substrates or the performance of ligand accelerated catalysis,[3] but severly restricts the potential of $^{63/65}$Cu NMR. Therefore, the NMR structural investigations, which are possible for these complexes, are limited to the NMR active nuclei of ligands or substituents. Another characteristic feature of these copper complexes with lower coordination numbers is the potential self-aggregation into dimeric, oligomeric, and polymeric structures.[21–24] For organocuprates, which are generally accepted as mechanistic models for organocopper chemistry, a number of theoretical[22,25–28] and experimental investigations[23,24,29] have shown that these aggregated species are most likely more than unreactive resting states in solution. The reactivity and the synthetic potential of copper(I) complexes or metal organocuprate clusters were supposed to be based on the ability of these complexes to form supramolecular assemblies of a size that is appropriate to allow cooperative interactions within the polymetallic cluster and the formation of open conformations.[22] The complicated structure determination of these aggregated species in solution, the existence of dynamic equilibria between several species, and the resulting sensitivity of the reaction to solvent and salt effects have so far been a hindrance to a rational design capable of tapping the full potential of copper reagents. Beside the fact that the structure elucidation of such aggregated complexes still remains a real challenge, the continually improving NMR methodology and, in particular, the application of diffusion ordered spectroscopy (DOSY for reviews see refs 30–37), has recently given some insight into the structures of copper complexes in solution.

After an overview of the principles and the application range of $^{63/65}$Cu NMR in section 2, the main part of the review deals with the structures of organocuprate reagents and intermediates in solution (see section 3). In particular, the structure determination of dimethylcuprate aggregates and intermediates in solution is described, as they have been investigated in the greatest detail so far. In addition, dimethylcuprates are used as model systems in theoretical calculations investigating the reaction pathways of organocuprates. Completing the organocopper section, the recent progress in amidocuprate structures is described. Recently, the first structures of chiral copper complexes and precatalysts in solution were reported, allowing impressive new insights into the structural diversity of synthetically famous copper catalyzed addition reactions. Therefore, in section 4, the NMR approaches and the resulting structures of copper complexes with TADDOL-like thiol ligands and phosphoramidite ligands are described. Furthermore, the progress in structure eludication of copper complexes with ferrocene-derived diphosphine and diimine ligands is presented.

2. ^{63}Cu and ^{65}Cu NMR Spectroscopy

2.1. General Applicability

Given the enormous success of NMR of metals (for some recent reviews, see refs 38–48) for structural characterization of important inorganic materials, organometallic molecules, and biological systems, the use of copper NMR should have the greatest potential for studying diamagnetic copper complexes, but its scope of practical application is severely limited. The two NMR active isotopes, ^{63}Cu and ^{65}Cu (both $I = 3/2$), have quite high natural abundances of 69.1 and 30.9% combined with magnetogyric ratios (γ) similar to ^{13}C ($\gamma(^{63}\text{Cu}) = 7.1088 \cdot 10^7$ rad T^{-1} s^{-1}, $\gamma(^{65}\text{Cu}) = 7.6104 \cdot 10^7$ rad T^{-1} s^{-1}, $\gamma(^{13}\text{C}) = 6.7283 \cdot 10^7$ rad T^{-1} s^{-1}). This combination results in promisingly good receptivities with respect to ^{13}C ($D^C(^{63}\text{Cu}) = 382$ and $D^C(^{65}\text{Cu}) = 298$).[49] However, the large quadrupole moments of ^{63}Cu and ^{65}Cu ($Q^{63}\text{Cu} = -0.220 \cdot 10^{-28}$ m^2 and $Q^{65}\text{Cu} = -0.204 \cdot 10^{-28}$ m^2) have largely prohibited routine NMR experimentation. In solid state NMR, the central transition powder patterns can be in the order of MHz in breadth,[50] and in high resolution NMR, even small electric field gradients at the nucleus lead to line widths in the kHz range or beyond detectability due to effective quadrupolar relaxation.[51–55] In the solid state, nuclear quadrupolar resonance (NQR) has been successfully used to probe copper sites of low symmetry in inorganic salts,[56] copper halides,[57–61] high temperature superconductors,[62–65] and magnetic materials.[66–69] Recently, frequency-stepped $^{63/65}$Cu solid state NMR experiments were shown to provide rapidly aquired $^{63/65}$Cu NMR spectra[70] for a variety of inorganic copper(I) complexes with large quadrupolar interactions.[50] In contrast, in solution NMR, it has not been possible up to now to deal with large quadrupole moments in a satisfactory manner. Thus, the observation of any $^{63/65}$Cu signal is limited to very small electric field gradients at the copper nucleus, which result from a high symmetry of its environment.[20] Consequently, mainly $^{63/65}$Cu spectra of copper (I) complexes with rigorous T_d symmetry, such as CuL_4-type complexes, have been reported so far. In case L represents a P-donor ligand, often even well-resolved scalar coupling patterns are observed in the $^{63/65}$Cu and ^{31}P spectra (see Figure 1a and b). $^{63/65}$Cu signals of complexes with reduced symmetry, such as CuL_3L'- and $CuL_2L'_2$-type complexes, are extremely broad (see Figure 1c) and frequently not even detectable, except for certain copper complexes with one CO ligand (see below). To my knowledge, there are no reports in which $^{63/65}$Cu NMR spectra of trigonal and linear copper(I) complexes have been

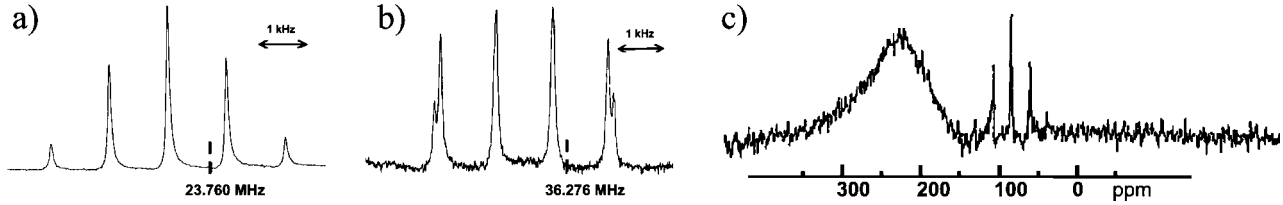

Figure 1. Typical ^{63}Cu (a) and ^{31}P (b) NMR spectra of a $[CuL_4]^+$ cation with P-donor ligands and a regular tetrahedral coordination of copper. The ^{63}Cu spectrum shows a quintet caused by $^1J_{Cu,P}$ couplings to the four P-donor ligands, the ^{31}P spectrum shows a quartet of equal intensities from $^1J_{Cu,P}$ to ^{63}Cu ($I = 3/2$) with the ^{65}Cu ($I = 3/2$) splittings visible on the external lines. Reprinted with permission from ref 51. Copyright 1982 Elsevier. (c) Line broadening of ^{63}Cu signals due to reduced symmetry. The sharp signal at 89.5 ppm is characteristic for tetracoordinate $[Cu(P(OC_2H_5)_3)_4]Cl$, the signal at approximately 250 ppm is attributed to a lower symmetry complex. Reprinted with permission from ref 77. Copyright 1982 Elsevier.

successfully detected in solution. On the other hand, tetrahedral copper(I) complexes, even in binary or ternary ligand systems, possibly yield detectable signals.[71,72] Despite these inherent restrictions to highly symmetrical Cu(I) complexes in solution, there are some review articles on $^{63/65}$Cu NMR[53–55,73] and a number of $^{63/65}$Cu spectra of Cu(I) complexes with various ligands, for example, phosphites,[20,51,72,74–78] phosphines,[75,79,80] diphosphines,[80–86] phosphaadamantanes,[87] nitriles,[20,71,72,74,78,88–97] derivatives of pyridine,[78] borates,[98] bisseleno- and bistelluroethers,[99] arsenic and antimony donor ligands,[80] and carbonyl compounds.[55]

2.2. Structural Information Available from $^{63/65}$Cu NMR Spectra

From $^{63/65}$Cu NMR studies and related investigations published so far, a couple of valuable structural parameters about copper complexes in solution have been gathered. For example, the π-acceptor properties of the copper bound ligands or vice versa the extent to which the copper ion can donate electrons to these ligands, have been measured based on ^{63}Cu NMR. This is possible because ^{63}Cu chemical shifts are primarily determined by the back-donation of electrons from the copper *d* orbitals to the ligands.[100,101]

From the line width of the ^{63}Cu signals and its temperature dependence, information about the symmetry of the copper complex and the ligand exchange rate can be obtained. In the absence of ligand exchange contributions, quadrupolar relaxation is dominant and the ^{63}Cu line width indicates the symmetry of the electric field around the copper nucleus.[51,88,100] In this quadrupolar relaxation regime, ^{63}Cu NMR signals become sharper with increasing temperature (see Figure 2), as generally known for NMR signals of isotopes with $I > 1/2$. Other important factors, such as viscosity and concentration of the sample, were shown to affect the line width by modifying the molecular rotation of the copper complex, expressed by the so-called correlation time.[88] In some complexes, ion pairing effects also contribute to line broadening.[88]

The theoretically clear correlation between a symmetric tetrahedral coordination of $[CuL_4]^+$ complexes and small line widths of their ^{63}Cu NMR signals was experimentally confirmed for copper(I) phosphite complexes by EXAFS data.[78] According to the lengths of the multiple Cu−P−P scattering pathways, the complexes with large line broadening in the copper NMR spectra were found to deviate more from a regular tetrahedron than complexes with sharper $^{63/65}$Cu NMR signals. For complexes with triphenyl phosphite and tri*n*-butylphosphine ligands, no ^{63}Cu NMR signals could be detected, contrary to what was expected. This was attributed to angular distortions leading to deviations from tetrahedral symmetry, because EXAFS data showed that the Cu−P bond lengths and their distribution were in accordance

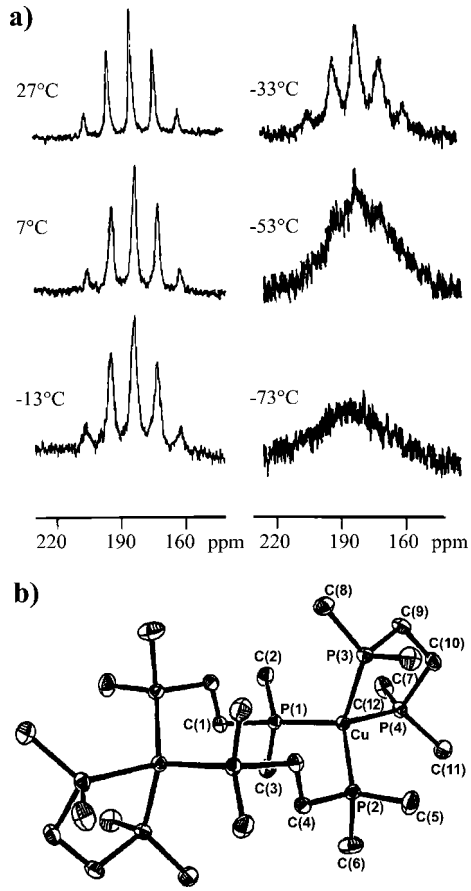

Figure 2. Variable-temperature ^{63}Cu NMR spectra (a) and molecular representation of the crystal structure (b) of $[Cu(1,2\text{-bis(dimethylphosphino)ethane})_2]_2^{2+}$ as example for a dimeric Cu(I) complex with tetrahedral coordination around each copper atom in the quadrupolar relaxation regime, which is indicated by the decrease in ^{63}Cu line widths with increasing temperature. Reproduced with permission from ref 83. Copyright 1991 American Chemical Society.

with a tetracoordinate tetrahedral structure and similar to the other complexes with detectable ^{63}Cu NMR signals. Interestingly, in this combined NMR/EXAFS study,[78] it is mentioned that in general the copper phosphite complexes investigated in solution seem to deviate slightly more from a regular tetrahedron than the corresponding complexes in the solid state. This tendency is also confirmed by our studies about precatalytic copper phosphoramidite complexes (see section 4.3).

Besides quadrupolar relaxation, dynamic processes occurring in solution are the second main factor affecting the line widths of ^{63}Cu NMR signals.[51,53,88,100] The nature and rate of these exchange processes are in turn influenced by

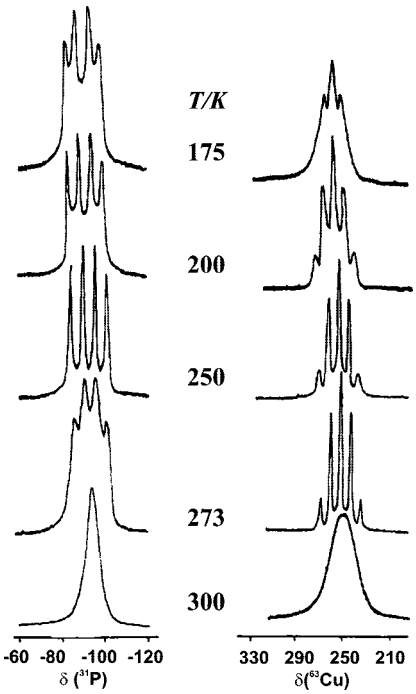

Figure 3. Variable-temperature $^{31}P\{^{1}H\}$- and ^{63}Cu NMR spectra of $[Cu(PPhH_2)_4]^+$.[80] Both signals show line width minima indicating that mainly quadrupolar relaxation is dominant at low temperatures and ligand exchange processes start to contribute at higher temperatures. Reprinted with permission from ref 80. Copyright 1993 Royal Society of Chemistry.

temperature as well as the electronic and steric properties of the ligands. As soon as ligand exchange processes occur in copper complexes, the ^{63}Cu NMR line width increases with rising temperature.[51,88,102] In particular, spectroscopically unresolved exchange processes with complexes of lower symmetry broaden the observed $^{63/65}Cu$ NMR signals. These complexes are usually generated by ligand dissociation and very short quadrupolar relaxation times can be assumed. Studies on tetrahedral Cu(I) complexes with phosphite-[51] and phosphine-ligands[79,103,104] revealed that the amount of complex dissociation in solution increases with Tolman's cone angle, which is a measure for the size of these ligands.[105,106] The activation energies for reorientation and exchange processes of the phosphite ligands in $[Cu(P(OCH_3)_3)_4]^+BF_4^-$ in CD_2Cl_2 were, for example, 12.6 and 17.7 kJ/mol,[51] respectively, and corresponding results were reported for $[Cu(P(OCH_2CH_3)_3)_4]^+BF_4^-$[51] and $[Cu(NCCH_3)_4]^+$.[88] Considering the temperature dependence of the quadrupolar relaxation mechanism combined with that of the ligand exchange processes, line width minima were often detected in the $^{63/65}Cu$ and ^{31}P NMR spectra of Cu(I) complexes (e.g., see Figure 3).[51,53,80,88] In general, a larger number of $^{63/65}Cu$ signals were detected in Cu(I) complexes with P donor ligands[53,88] than with N donor ligands, due to a reduced exchange tendency of P donor ligands. This is in agreement with theoretical calculations on $[Cu(PH_3)_4]^+$ revealing a lower degree of dissociation for the third and fourth phosphine ligands[107] compared to ammine ligands in $[Cu(NH_3)_n]^+$ ($n = 1-4$).

Quite recently, an interesting approach to sharpen the ^{63}Cu NMR signals was published, in which CO was used as ligand in copper(I) complexes with various tridentate N-donor ligands.[98,100] The π-acceptor properties of CO as ligand in these Cu(I) complexes coincidentally cancel the donor effect of the tridentate N-donor ligand. This effect changes the expected asymmetric charge distribution around the copper ion into a more symmetric one. The resulting reduced electric field gradient at copper leads to a slow quadrupolar relaxation and sharp ^{63}Cu NMR signals (see Figure 4). This concept of matched donor and acceptor effects of the ligands in Cu(I) complexes seems promising, especially if it becomes applicable to various ligand systems. Nevertheless, to investigate the structure of Cu(I) complexes in solution, the application of $^{63/65}Cu$ NMR spectroscopy is still strongly limited to complexes with a highly symmetrical tetrahedral coordination around copper and particular ligand systems.

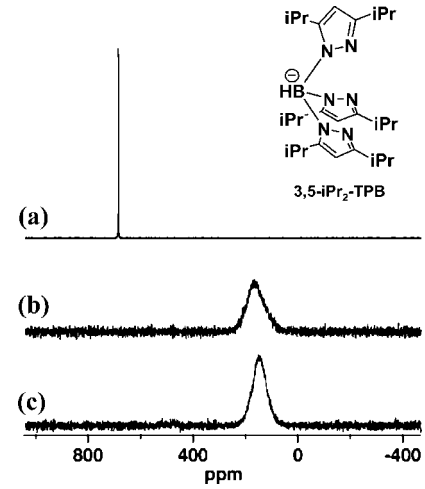

Figure 4. Very sharp ^{63}Cu NMR signal of (a) (3,5-*i*-Pr_2-TPB)CuCO in CD_2Cl_2 compared to the signals of (b) (3,5-*i*-Pr_2-TPB)Cu(CH_3CN) in CD_3CN, and (c) (3,5-*i*-Pr_2-TPB)Cu(PPh_3) in CD_3CN show the significant reduction of the electric field gradient around copper due to a matched donor acceptor ligand pair.[100] For clarification, a schematic representation of the ligand 3,5-*i*-Pr_2-TPB is given. Reprinted with permission from ref 100. Copyright 2007 American Chemical Society.

3. Structure Determination of Organocuprates in Solution

3.1. Introduction

Perhaps the most famous example of the efforts and difficulties in elucidating structures or reaction intermediates of copper reagents in solution is the extensive and still ongoing discussion about the structural aspects of organocuprates and particularly those of cyanocuprates.[22,24,26–28,108–121] Because organocuprates are among the most frequently applied transition metal reagents for the formation of C−C bonds in organic synthesis,[3,122–124] numerous structural studies have been published and there are some comprehensive articles and several book chapters summarizing the combined efforts of spectroscopic methods, X-ray crystallography, and theoretical calculations up to the years 2000/2002.[3,22,115,125,126] Therefore, this review focuses on NMR investigations of organocuprates in solution and places the main emphasis on recent developments. Moreover, some previous studies and the required background information are provided to clarify the underlying spectroscopic approach.

In the structure elucidation of organocuprates and cyanocuprates, the monomeric species have raised the famous discussion about the existence of "higher order" cuprates ($R_2Cu(CN)Li_2$)[127–129] beside cyano-Gilman cuprates ($R_2CuLi{\bullet}LiCN$) and heteroleptic cyanocuprates (RCu(CN)Li) in solution.[115] The main cause for this controversy is the

complicated accessibility of structural information on diorganocuprates in solution. The high symmetry of the diorganocuprates reduces the number of NMR signals rigorously, for example, in the model system for dialkylcuprates, $Me_2CuLi{\bullet}LiX$ (X = Cl, Br, I, CN), only one signal is detectable per element (^1H, $^{6/7}Li$, and ^{13}C). Moreover, scalar coupling patterns to the metals Cu and Li would reveal valuable structural information, but they are usually not detectable in diorganocuprates. From a series of crystal structures, it is known that organocuprates with the stoichiometry $[R_2CuLi]$ and $[R_2CuLi_2X]$ (X = Cl, Br, I, CN) have mostly a linear Cu coordination in the solid state (see Figure 5a−f).[23,120,130–136] Other arrangements are observed only with additional donor ligands or aromatic moieties comprising donor moieties.[136] Due to the fast quadrupolar relaxation of the copper isotopes in complexes with a coordination number lower than four (see section 2), it is not possible to determine the number of substituents on copper in organocuprates from scalar coupling patterns to $^{63/65}Cu$ as it is possible for transition metals such as ^{195}Pt, ^{103}Rh, or ^{109}Ag with $I = 1/2$.[40,43,44,137] Neither are $^{6/7}Li-^{13}C$ scalar couplings detected in lithium dialkylcuprates,[29,113,138–140] which was attributed to a fast exchange of the lithium ions.[138] In our investigations of the ion pairing equilibria in solution,[140] we found that even the $^1J_{1H\text{-}13C}$ scalar coupling of $[Me_2CuLi]$ is not affected by the formation of contact ion pairs (CIPs) or solvent separated ion pairs (SSIPs), which may be explained by theoretical calculations showing mainly ionic interactions of lithium.[141] In contrast, in amido cuprates, where one of the reactive organo groups is replaced by a nontransferable amido group (and sometimes also in diarylcuprates), the situation of binding and exchange is significantly different. This favors amidocuprates as it results in well resolved $^{6/7}Li-^{15}N$ scalar couplings and sometimes even in detectable $^{6/7}Li-^{13}C$ scalar couplings.[142–145] The detection of scalar couplings to lithium allows for a structure elucidation process of amidocuprates in solution similar to that of organolithium compounds or lithium complexes with chiral amine ligands. For these lithium compounds scalar couplings and nuclear Overhauser effects are widely used to determine their aggregation and structure in solution.[146–154] Thus, the different binding and exchange situations in dialkylcuprates and in amidocuprates necessitate fundamentally different NMR spectroscopic approaches. Therefore, the structure elucidation of diorganocuprates as free reagents and in reaction intermediates is described first in section 3.2; subsequently, the structure determination of amidocuprates is addressed in section 3.3.

3.2. Diorganocuprates

3.2.1. Monomer Structure

The comparison of $^{13}C-^{13}C$ scalar coupling constants and multiplicity patterns in model cuprates with and without cyanide moieties was one of the most substantial arguments to decide the discussion about the structure of cyanocuprates in solution in favor of the cyano Gilman cuprates. Fortunately, the line broadening effect of $^{63/65}Cu$ on the ^{13}C resonances is small enough to allow the direct detection of two bond $^{13}C-^{13}C$ and three bond $^1H-^{13}C$ scalar couplings across copper in ^{13}C labeled or partially ^{13}C labeled monomeric cuprates in THF (see Figure 6).[113,139] For aggregated species in diethyl ether, only temperatures of ≤173 K or additives causing disaggregation such as hexamethylphosphoramide (HMPA) or crown ethers (12-crown-4) produce line widths sufficiently narrow enough to enable the direct determination of $^2J_{C,C}$ and $^3J_{H,C}$ coupling constants from multiplicity patterns in one-dimensional ^{13}C spectra.[139] With the aid of these scalar coupling constants across copper, it was concluded that the "dimethylcuprate core" in

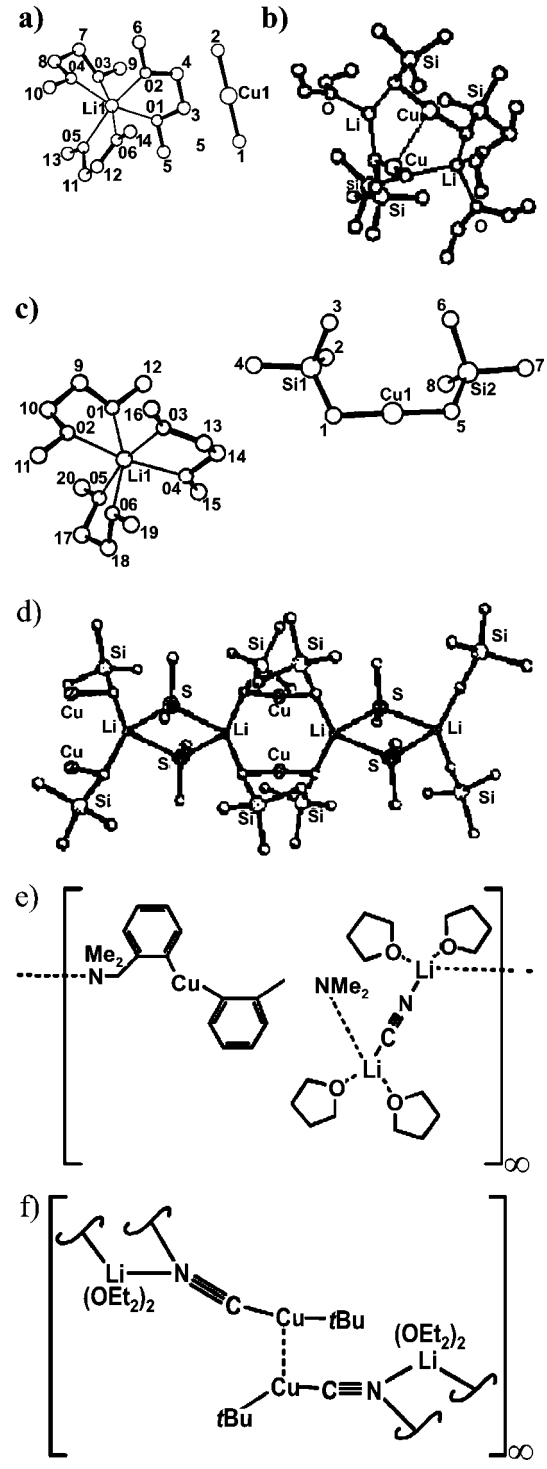

Figure 5. In organocuprates, the mostly linear coordination of copper and the different levels of aggregation are shown by the solid state structures of (a) $[Li(dme)_3]^+[Me_2Cu]^-$,[23] (b) $[Li_2Cu_2(CH_2SiMe_3)_4(Et_2O)_3]$,[23] (c) $[Li(dme)_3]^+[(Me_3Si)CH_2\}_2Cu]^-$,[23] and (d) $[Li_2Cu_2(CH_2SiMe_3)_4(SMe_2)_2]_\infty$[155] and the structure schemes of (e) $[(2\text{-}(Me_2NCH_2)C_6H_4\}_2CuLi_2(CN)(THF)_4]_\infty$[134] and (f) $[t\text{-}BuCu(CN)Li(OEt_2)_2]_\infty$.[135] Reprinted with permission from ref 24 and ref 23. Copyright 2003 American Chemical Society and 2000 Wiley VCH.

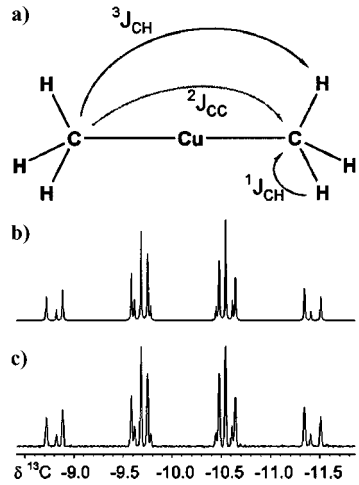

Figure 6. In monomeric cuprates or at very low temperatures scalar couplings across copper can be detected in one-dimensional ^{13}C spectra to specify the type and number of substituents on copper as shown for the $A_3XX'A_3'$ spin system of a dimethylcuprate core; (a) scheme with the observed scalar couplings, (b) simulated, and (c) experimental ^{13}C spectrum of Me_2CuLi in THF. Reprinted with permission from ref 113. Copyright 1998 American Chemical Society.

$Me_2CuLi{\bullet}LiCN$ is the same as in "halide-free" Me_2CuLi and that the CN^- group is not directly bound to copper in $R_2CuLi{\bullet}LiCN$ compounds. These results were in agreement with the interpretations of ^{13}C- and ^{15}N chemical shift data of several cyanocuprates,[108,138] EXAFS- and XANES studies,[141,156,157] quantum chemical calculations,[158–160] as well as crystal structures of cyanocuprates with 2:1 stoichiometry[134,135] to specify only some of the arguments,[115] which helped to finalize the discussion on the monomeric structure of cyanocuprates in favor of the cyano Gilman cuprates $R_2CuLi{\bullet}LiCN$. Later on, cyanocuprates with CN^- and more than one additional organic substituent directly bound to copper were only proposed for intermediate π-complexes in theoretical studies[28] and experimentally detected in square planar Cu(III) intermediates (see section 3.3.3).

3.2.2. Monomer/Dimer Equilibria

Long before cluster formation and aggregation of organocuprates were known to be a decisive factor for their reactivities, early colligative measurements of dimethylcuprates in diethyl ether suggested the formation of dimers.[161,162] In addition, a strong influence of the solvent[163] or lithium coordinating additives[164] was observed from the reactivities of organocuprates. The conjugate addition reaction of organocuprate reagents with enones is much faster in less polar solvents such as dichloromethane,[165] hydrocarbons,[165] and dimethylsulfide[166] than in more polar solvents such as THF or pyridine.[165] In contrast, the reaction of organocuprates with alkyl halides is much faster in polar solvents.[163,167] Later on, more information was gathered on different possible aggregation levels of organocuprates. For example, theoretical calculations proposed the dimer to be the minimal cluster size for reactions of organocuprates.[22,25,26,168] Ebullioscopic measurements suggested dimers in THF[162] and broad line widths of ^{13}C and ^{15}N signals[138] as well as results of electrospray ionization mass spectrometry[169] indicated aggregation in diethyl ether. Crystal structures also show that the R-Cu-R^- unit exists in different arrangements such as monomeric solvent-separated ion pair type structures,[23,131,135,170] dimers,[23,155,171–173] and polymeric chains[134,135] (for selected examples see Figure 5). From these crystal structures, it was deduced that $R_2CuLi{\bullet}LiX$ crystallizes in a solvent separated ion pair structural type from solvents, which coordinate well to Li^+ (e.g., THF), or in presence of strongly coordinating additives (e.g., [12]crown-4 or amines).[23] In contrast, solvents with poor donor qualities for Li^+ (e.g., diethyl ether or dimethyl sulfide) lead to solid state structures of the contact ion pair type.[23] In solution, the aggregation level of organocuprates was unclear for a long time. Only for phenylcopper and diphenylcuprate was it possible to detect separated sets of ^{13}C signals for differently aggregated species, which could be used to identify monomers, dimers, trimers, and tetramers via comparisons with known crystal structures as well as temperature and concentration dependent trends of lithium reagents.[174]

A direct transfer of the very valuable structural information from crystal structures and theoretical calculations to the situation in solution has to be performed with great caution. Crystal packing effects may change the relative energies of different conformations and in theoretical calculations it is still difficult to include the contribution of a larger cluster and/or solvent shell. In the case of lithium enolates for instance, D. B. Collum stated that "one cannot infer from crystal structures the dominance or even the existence of these forms in solution" and that "the solution aggregation numbers must be determined independently".[175] This statement was based on structural studies, in which species undetectable in solution were characterized crystallographically.[176–178] On the other hand, for dialkylcuprates in solution it is not possible to apply a classical NMR structure elucidation approach using scalar couplings and nuclear Overhauser effects (NOEs) for quantitative angular and distance restraints. The symmetry of the aggregates combined with exchange processes minimizes the number of detectable NMR signals, for example, in oligomeric $Me_2CuLi{\bullet}LiX$ only one ^1H, ^{13}C, and $^{6/7}Li$ signal is detected. In addition, the sparse homonuclear NOEs represent the sum of distances between chemically equivalent moieties. Scalar couplings are only detectable within monomeric R−Cu−R units, and diffusion coefficients only yield the hydrodynamic radius, that is, the size of an aggregate, but not its structure. Therefore, following the classical NMR approach, based exclusively on NMR parameters, the structures of dialkylcuprates in solution are absolutely underdetermined. Despite this situation, it is possible to extract decisive parameters for different structural arrangements from known crystal structures and theoretical calculations, measure these parameters by tailored NMR experiments and thus, step by step, elucidate the structure of these aggregates in solution.

Considering the crystal structures of organocuprates (for selected examples see Figure 5) an eye-catching parameter proves the existence of solvent separated ion pairs (SSIPs) (Figure 5a, b) and contact ion pairs (CIPs) (Figure 5c−f). SSIPs and CIPs show notably different distances between the protons of the cuprates and the lithium ions of more than 500 pm and less than 250 pm, respectively.[140] In solution these ^1H-$^{6/7}Li$ distances can be visualized using ^1H-$^{6/7}Li$ HOESY experiments,[179–189] which show strong cross-peaks for distances around 250 pm and have an upper limit for detectable direct interactions of 400−500 pm.[186,190–192] Indeed, for the salt-free Me_2CuLi in diethyl ether, a strong cross-peak between lithium and the CH_3 groups of the cuprate is seen in the $^1H-^6Li$ HOESY spectrum (see Figure 7b), indicating that the main species in solution is a contact

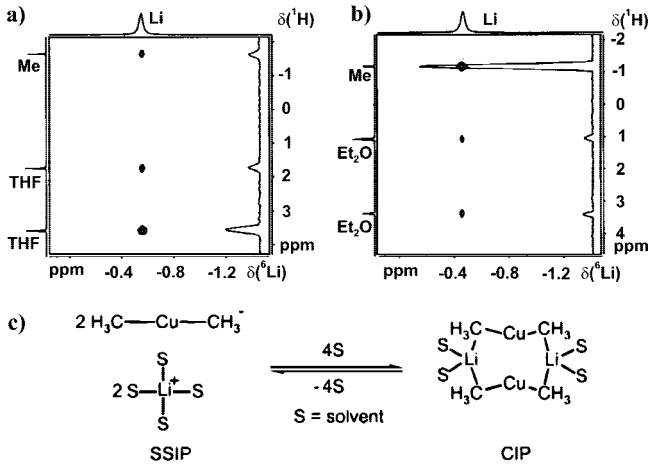

Figure 7. $^{1}H-^{6}Li$ HOESY spectra of Me_2CuLi in (a) THF and (b) diethyl ether as well as (c) a model of a CIP-SSIP equilibrium between monomeric and dimeric Me_2CuLi. The intensities of the Me/Li cross-peaks in (a) and (b) monitor the position of the CIP-SSIP equilibrium. Reprinted with permission from ref 140. Copyright 2000 American Chemical Society.

ion pair.[140] For Me_2CuLi•LiCN and Me_2CuLi in THF, only a weak dipolar interaction between lithium and the CH_3 groups was observed (see Figure 7a). To interpret this small cross-peak in terms of structural information it is of great importance to exclude all other possibilities apart from a direct dipolar transfer. $^{1}H-^{6}Li$ HOESY spectra of MeCu(CN)Li and *t*-Bu_2CuLi•LiCN in THF confirmed that in pure SSIPs a corresponding cross-peak is not detectable. In addition, using different experimental setups, contributions from other magnetization transfers were excluded such as: indirect transfer pathways via the solvent molecules, chemical exchange, influences of different correlation times or the existence of background signals. By proving that these dipolar interactions represent a direct transfer, it became evident that they reveal an equilibrium between SSIPs and CIPs of dialkylcuprates in solution with the CIPs as minor species in THF and as major species in diethyl ether (see Figure 7c).[140] The results of these $^{1}H-^{6}Li$ HOESY experiments from the ion pairing of organocuprates in solution corresponded perfectly with Bertz's logarithmic reactivity profiles of reactions of R_2CuLi with enones in diethyl ether and THF[163,193] and the suppression of this reaction by crown ethers.[164] Therefore, these investigations allowed the first structure reactivity correlation of dialkylcuprates in conjugate addition reactions to enones. The fast reaction in diethyl ether was attributed to the predominance of CIPs as the reactive species. In THF only a small amount of CIPs is present as reactive species in fast equilibrium with the SSIPs resulting in a much slower reaction (see Figure 8).

3.2.3. Structure of the Dimeric Core Unit

The structure elucidation of organocuprate CIPs in solution has gained importance after their identification as reactive species in conjugate addition reactions. The influence of the CN^- group on the structure of the aggregates is especially interesting in terms of the previous discussion about "higher order" cuprates. Again, it is crucial to identify NMR accessible parameters within the different proposed aggregate structures and their measurement in appropriate model systems. For salt-free Me_2CuLi in diethyl ether, various studies (crystallographical studies of similar compounds,[23,155] quantum chemical calculations[22,25,26,194,195] and colligative measurements[111,162,196]) consistently indicate a homodimeric structure (see Figure 9). Recently, homodimeric structures were also proposed for the homoarylcuprate $[Cu_2Li_2Mes_4]$ (Mes = 2,4,6-$Me_3C_6H_2$) in toluene, the structural information being mainly based on crystal structures.[197] In contrast, the structure of the CIPs of salt-containing Me_2CuLi•LiCN represents a rather inconsistent picture. EXAFS,[114] infrared studies in THF,[198] most of the theoretical calculations,[22,141,158,159] and X-ray studies with special diamine arylcuprates[120,199] indicate heterodimeric core structures (see Figure 9). However, in most of the compounds crystallized from LiX containing solutions (X = Br, CN), the presence of a LiX moiety was not observed in the solid state structure, and a homodimer was obtained as the basic structural element.[23,155] In addition, equilibria have been suggested between homodimeric and heterodimeric structures in solution, with the homodimer as the main contributor.[195]

In Figure 9, the characteristic distances of homodimeric and heterodimeric core structures of the model system Me_2CuLi•LiCN and the resulting theoretical ^{1}H, ^{1}H NOE and ^{1}H, ^{6}Li HOE ratios are given (4.3 and 2.2, respectively). These ratios, especially the one for ^{1}H, ^{1}H NOE, are suited as clear decision criteria for homodimeric or heterodimeric core structures. Salt-free Me_2CuLi in diethyl ether can be used as an ideal model system for homodimeric CIPs in solution, whereas Me_2CuLi•LiCN is suitable to test the existence of heterodimers. However, it is necessary to overcome some obstacles to quantify the dipolar interactions within these two model systems. In general, known distances within the molecules are used as reference values for the quantification of dipolar interactions. This technique has a great advantage in that it renders the determination of correlation time redundant.[187,192] However, in dimethylcuprates there is no fixed and known distance, which can be used as reference value. Thus, the correlation time (affecting ^{1}H, ^{1}H NOE and ^{1}H, ^{6}Li HOE differently) has to be determined for each compound separately to quantify the ^{1}H, ^{6}Li HOE buildup curves (for details see Gschwind et al.).[112] In addition, due to the symmetry of homo- and heterodimers the ^{1}H, ^{1}H NOE has to be measured between chemically equivalent protons. The different isotopomers $^{1}H-^{13}C$ and $^{1}H-^{12}C$ can be used to overcome this symmetry problem by breaking the chemical equivalence (see Figure 10a). Usually HMQC-ROESY[200] and HSQC-NOESY[201] pulse sequences are applied for this purpose. Both of these experiments were found to be too insensitive to observe any NOE between the cuprate isotopomers, even with 20% ^{13}C labeled cuprate samples. A thorough analysis of these experiments revealed that the positioning of the two coherence selecting pulsed field gradients on both sides of the mixing time cause severe intensity attenuation due to self-diffusion of the molecules during the mixing time.[202] With the appropriate change to NOE-HSQC and ROE-HSQC sequences[202] very similar ^{1}H, ^{1}H NOE-HSQC buildup curves of Me_2CuLi and Me_2CuLi•LiCN were detected (see Figure 10b) and the difference in correlation time was shown to be negligible by the application of ^{1}H, ^{1}H ROE-HSQC spectra.[112]

Thus, the similar ^{1}H,^{1}H dipolar interactions in Me_2CuLi and Me_2CuLi•LiCN as well as the H−Li distances in these cuprates indicate the presence of a homodimeric core structure for both compounds in diethyl ether.[112] This is in agreement with the previously proposed structure of the reactive CIP (see Figure 8). A later study of the control of

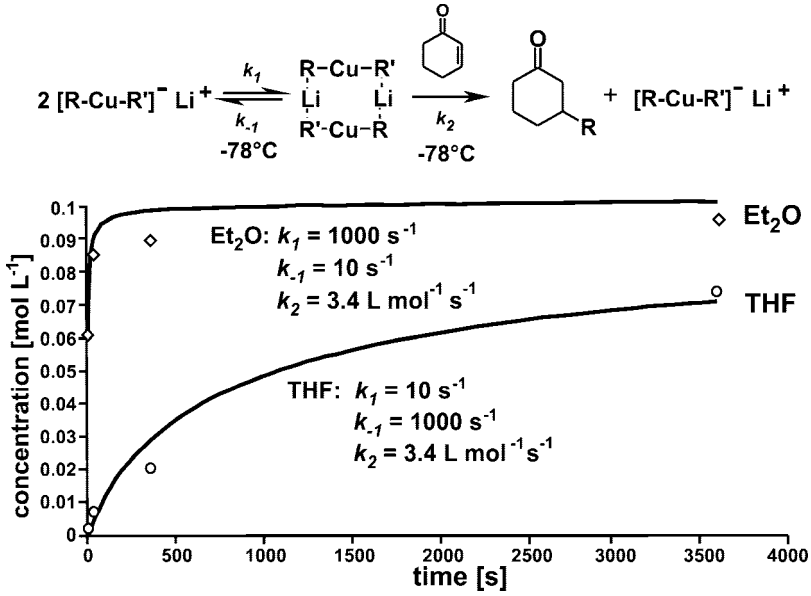

Figure 8. Equilibrium between SSIPs and CIPs in solution with the CIPs as reactive species in conjugate addition reactions. Corresponding logarithmic reactivity profiles (LRPs) of the reactions of $BuCu(SSiMe_3)Li•LiI$ with cyclohexenone in diethyl ether (Et_2O) and THF at −78 °C. Points: experimental values and curves: theoretically calculated with the rate constants given. Reprinted with permission from ref 23. Copyright 2000 Wiley VCH.

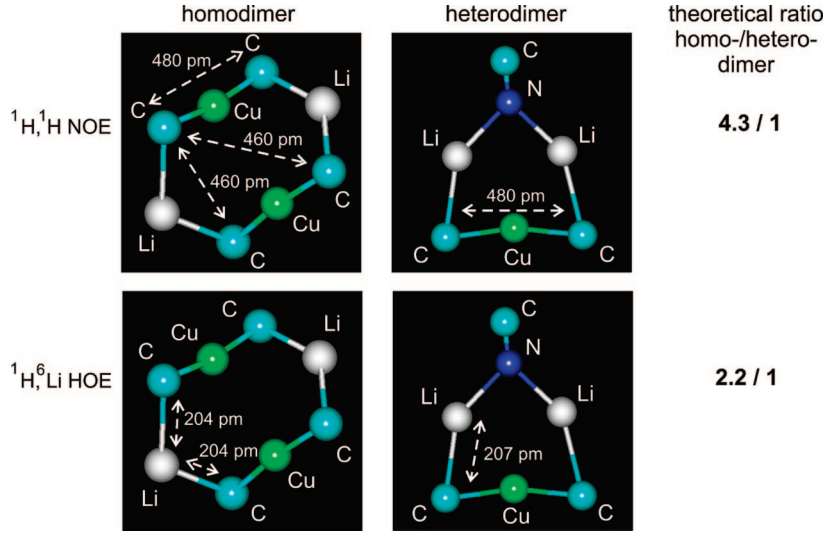

Figure 9. Differentiation between homodimeric and heterodimeric core structures of $Me_2CuLi•LiCN$ with the aid of homonuclear and heteronuclear NOEs. The numbers attached refer to the average distances in the two species and were used to calculate the given theoretical NOE and HOE ratios. Reprinted with permission from ref 112. Copyright 2001 American Chemical Society.

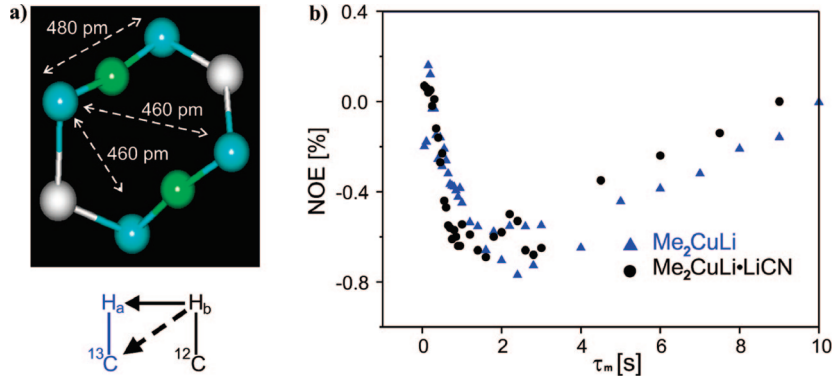

Figure 10. (a) ^1H, ^1H NOEs between chemically equivalent groups can be detected using the different isotopomers $^1H-^{13}C$ and $^1H-^{12}C$; (b) ^1H, ^1H NOE-HSQC buildup curves of Me_2CuLi and $Me_2CuLi•LiCN$ in diethyl ether show homodimeric core structures for both compounds. Reprinted with permission from ref 112. Copyright 2001 American Chemical Society.

electron transfer versus alkylation pathway of $Me_2CuLi•LiI$ showed as well that the lithium halide is similarly involved in the competition between these two reaction types.[203] With a special sample preparation and the utilization of ^{13}C labeled

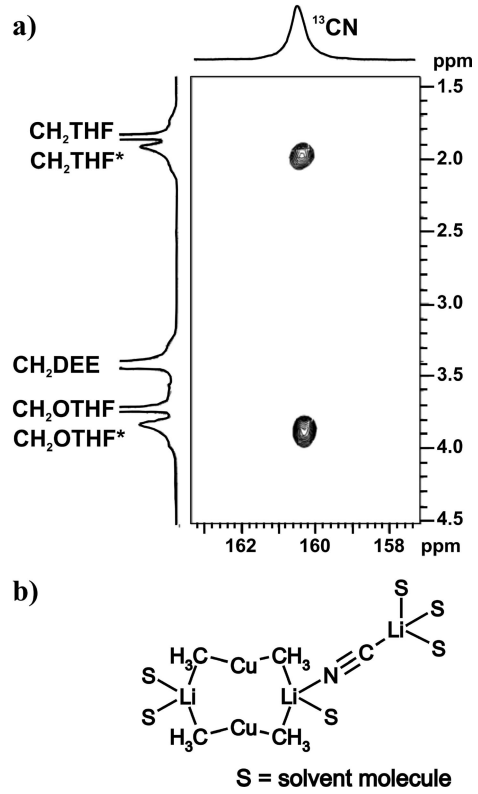

Figure 11. (a) ^{1}H, ^{13}C HOESY spectrum of Me_2CuLi•LiCN with 12 equiv of THF. Two sets of signals are observed for THF: in the solvent bulk (THF) and bound to the cuprate aggregate (THF*); the significant ^{1}H, ^{13}C HOE cross-peaks between THF* and CN^- indicates the orientation of CN^- shown in (b). Reprinted with permission from ref 29. Copyright 2005 American Chemical Society.

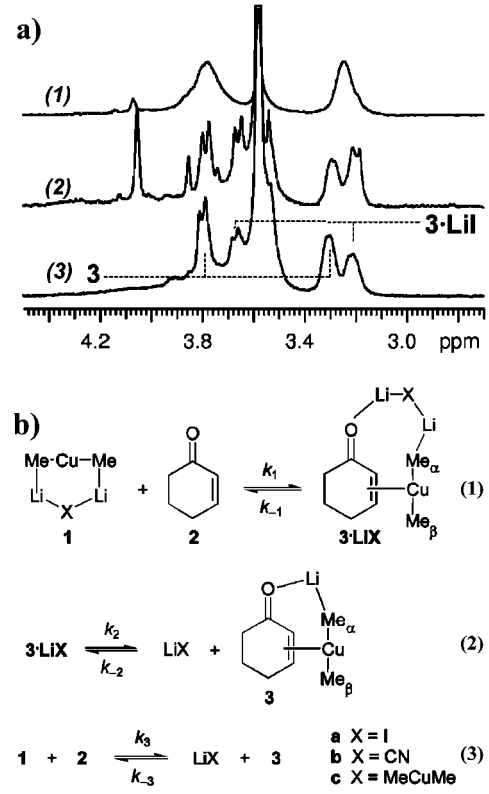

Figure 12. (a) ^{1}H NMR spectra of the π-complex vinyl region at 173 K and (b) the proposed equilibria of formation in THF. **3**•Li was identified in spectrum (2) by injecting LiI to (3). Samples with LiCN showed severe line broadening effects (1). Reprinted with permission from ref 121. Copyright 2005 American Chemical Society.

CuCN salt, we were later able to detect a direct ^{1}H,^{13}C HOE to the CN^- moiety in organocuprate aggregates for the first time.[29] This was possible because the fast exchange of the THF molecules is stopped and separate signals are detected for bulk THF and THF bound to the cuprate cluster (see Figure 11a). In spite of an extensive experimental effort the respective ^{1}H, ^{13}C HOESY spectrum shows only cross-peaks from CN^- to THF bound to cuprate but not to the methyl groups of cuprate (see Figure 11a). This further supports the homodimeric structure in diethyl ether and suggests an orientation of the CN^- group as shown in Figure 11b. Although this agrees with models from infrared spectroscopy[198] and EXAFS-data,[114] the shown orientation can not be postulated as fixed due to the relatively low isomerization barrier in LiCN[204] and known crystal structures.[205] In summary, the various experimental results for Me_2CuLi•LiCN in diethyl ether indicate a homodimer as the main species. Of course, this does not exclude the existence of heterodimers in minor conformations below the NMR detection limit or transition states as proposed, for example, in some theoretical calculations.[28]

In THF the structure elucidation of the CIP is even more complicated than in diethyl ether. Due to the fact that in THF the CIPs exist only as minor species at very low concentrations (see Figure 7 and 8), NMR spectroscopy is not sensitive enough for a direct structure elucidation as described for diethyl ether. Here, Bertz and Ogle found an elegant indirect method using the formation rates of π-complexes in THF.[121,206] With the aid of rapid-injection techniques,[207,208] they identified different π-complexes of Me_2CuLi•LiI and Me_2CuLi•LiCN with 2-cyclohexenone (see Figure 12a). Using exchange spectroscopy (EXSY)[192,209–211] and rapid -injection ^{1}H NMR data points for the reaction of Me_2CuLi•LiI with 2-cyclohexenone, the different rate constants for the equilibria shown in Figure 12b were determined. From the experimental results obtained and based on the assumption that the CIP is the reactive species,[23] they proposed a heterodimeric structure of the CIP in THF and the absence of homodimers in this solvent. However, considering the SSIPs as main species in solution the question remains whether additional equilibria (e.g., between the isolated cuprate monomer, the cuprate monomer with one lithium ion and the hetero- or the homodimer and between all of these four species and the enones) may contribute to the equilibira described above.

3.2.4. Oligomerization Trends

The cluster structure of organocuprates has been claimed to be essential for their reactivity.[22] As diethyl ether favors the formation of clusters in solution, this solvent offers a promising possibility to elucidate structure reactivity correlations. The so far described uniform homodimeric core structure explains neither the previously claimed higher reactivities of cyanocuprates[128] nor the differences in the relative reactivities of Me_2CuLi•LiI, Me_2CuLi•LiI•THF and Me_2CuLi•LiCN observed from logarithmic reactivity profiles (LRPs).[163] Hence, supramolecular structures of such organocuprate clusters beyond the dimeric core structure may cause these reactivity differences. In diethyl ether, the existence of aggregates larger than dimers is indicated by the negative sign of the ^{1}H,^{1}H NOE (see Figure 10b), broad line widths of ^{13}C and ^{15}N signals[138] as well as results of

Table 1. Diffusion Coefficients D (10^{-9}m^2 s^{-1}), Molecular Radii r_c (10^{-10} M)[a], Length Indices n and n_{mf}, Solvation Indices n_{solv}, and Theoretical Solvation Indices $n_{solv(t)}$ of Organocuprates in Diethyl Ether at 239 K[b]

complex	r_c[a,d]	D	n_{mf}[c]	n[d]	n_{solv}	$n_{solv(t)}$[d]
$(Me_3SiCH_2)_2CuLi$	5.39	0.59	1.3	1.7	4.8	3.2
$(Me_3SiCH_2)_2CuLi\backslash zmd\backslash LiI$	6.05 (6.39)	0.54	1.1	1.4 (1.3)	7.5	5.4 (7.5)
$(Me_3SiCH_2)_2CuLi\backslash zmd\backslash LiCN$	6.01 (6.35)	0.35	4.5	3.6 (3.2)	6.9	4.6 (6.6)
Me_2CuLi	4.22	0.53	4.4	3.1	2.4	2.6
$Me_2CuLi\backslash zmd\backslash LiI$	5.20 (5.64)	0.51	2.2	2.3 (1.9)	6.3	4.9 (7.0)
$Me_2CuLi\backslash zmd\backslash LiCN$	5.14 (5.58)	0.33	9.0	5.2 (4.5)	5.1	4.4 (6.4)

[a] r_c = radius of the core units calculated by molecular hard-sphere volume increments. [b] Reprinted with permission from ref.[24] Copyright 2003 American Chemical Society. [c] n_{mf} is the aggregation number calculated by a model-free approach (see text for details). [d] For salt-containing complexes, two sets of values are given: those obtained from model C (without brackets) and from model D (in brackets).

electrospray ionization mass spectrometry.[169] Therefore, it is highly desirable to gain information about the aggregation level and the structures of these higher aggregates.

Pulsed field gradient (PFG) diffusion NMR experiments offer a powerful tool to investigate the size of molecules including aggregates in solution,[30,31,36,37,189] which is more and more routinely applied to organometallic,[30,37,189] supramolecular,[35] and biomolecular[36] systems. The great advantage of this method compared to other colligative measurements is that the experimental parameters such as temperature or concentration can be adapted to the requirements. Mixtures of solvents or solutes do not form an obstacle either. The physical observable, easily derived from diffusion NMR experiments, is the translational self-diffusion coefficient, which in principle can be related to the size of the diffusing molecules by using several variations of the famous Stokes−Einstein equation. In a very recent review Macchioni et al. described in detail the general technical pitfalls including size- and shape-correction factors, which are associated with the accurate determination of hydrodynamic dimensions of molecular systems in solution.[30] Therefore, in this review, primarily these drawbacks and opportunities of diffusion measurements are outlined that are specific to organocuprates.

The measurements of accurate self-diffusion coefficients of organocuprates in solution by means of NMR require above all the elimination of convection contributions and the consideration of varying viscosities. For temperatures between 173 and 240 K, the effects of convection within the NMR tube can be completely eliminated by a pulse sequence developed by Jerschow and Müller.[212] In our laboratory, attempts have been made to replace this lengthy and insensitive pulse sequence by other shorter convection compensating pulse sequences[213] or to stop the convection by sample spinning. Both failed in the case of organocuprates in diethyl ether. Furthermore, to monitor changes in the viscosity, tetramethylsilane or benzene can be used as inert and not interacting internal standard.[24,214] With the aid of the described methods, accurate viscosity corrected self-diffusion coefficients of organocuprates in solution are obtained (see Table 1).

From the diffusion coefficients given in Table 1, it is evident that $(Me_3SiCH_2)_2CuLi$, $(Me_3SiCH_2)_2CuLi$•LiI, Me_2CuLi, and Me_2CuLi•LiI have similar hydrodynamic dimensions in solution despite the differences in the sizes of the two monomers. In contrast, the cyanocuprates $(Me_3SiCH_2)_2CuLi$•LiCN and Me_2CuLi•LiCN show a significantly higher aggregation level. Is it possible to connect these diffusion coefficients with the aggregation number n?[215] A reliable quantitative evaluation of diffusion coefficients in terms of aggregation numbers is always very critical because it requires a proper knowledge of the chemical

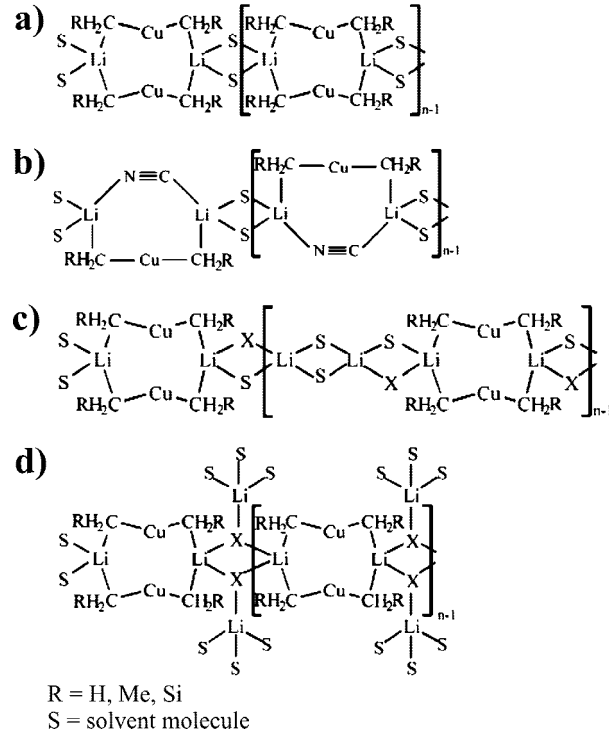

Figure 13. Structure models of dialkylcuprate aggregates beyond dimers: (a) salt-free homodimeric chain (model A), (b) salt-containing heterodimeric chain (model B), (c) and (d) salt-containing homodimeric chains (models C and D). Reprinted with permission from ref 24. Copyright 2003 American Chemical Society.

composition, the shape and the solvent shell of both the aggregate and the monomer and a careful consideration of exchange contributions. In general, the hydrodynamic radii of the elemental monomeric building blocks is experimentally determined via diffusion measurements of very diluted (i.e., disaggregated) samples.[30,216] However, a close inspection of the crystal structures showing monomeric, dimeric and polymeric organocuprates in the solid state (see Figure 5) indicates that the shape, size, and composition of monomeric, solvent separated cuprates differ too much from the polymeric systems to be suitable as elemental building blocks. Therefore, for salt-free organocuprate aggregates we used the known homodimeric core structures as elemental building blocks[22–24,112,155,194,195,217] and used the crystal structure of $[Li_2Cu_2(CH_2SiMe_3)_4(SMe_2)_2]$[155] as direct model for higher aggregates in solution (see Figure 13a and Figure 5d). For salt-containing cuprates in contrast, three different models were used as elemental building blocks. In agreement with the previous NMR studies, homodimeric core structures were chosen, which are connected over two different Li−X−Li salt bridges to build two models with homodimeric cores

(see Figure 13c and d). Even though less probable in diethyl ether, the possibility of heterodimeric core structures was still considered by connecting heterodimers, proposed in theoretical calculations, to a chain structure (see Figure 13b and Figure 9).

The crystal structures of the contact ion pairs show several solvent molecules attached to the organocuprate aggregate and it was shown for organolithium compounds that directly attached solvent molecules have to be included in the theoretical calculation of diffusion coefficients.[218] Therefore, to obtain reliable models, the average amount of solvent molecules attached to the cuprate cluster was determined experimentally by diffusion measurements (see Table 1), where the solvent molecules were found to be in the fast-exchange limit in the diffusion dimension.[219] The experimental number of solvent molecules attached was also the basis for the proposed salt bridge structures of the models shown in Figure 13c and d. Using hard sphere volume increments[220–222] for the core structures, the aggregation numbers n were calculated from these models and the corresponding shape factors (see Table 1 and ref 24 for further details). For maximum independency from the models used and for an estimation of the influence of the shape factors on n, a model free approach (n_{mf} in Table 1) was additionally calculated without shape factors in the Stokes−Einstein equation (i.e., application of a spherical shape). The numbers of n_{mf} and n in Table 1 show that the absolute numbers depend significantly on the model and the shape factor applied, but that the relative trends in aggregations are consistent for both shape factors. Later on, investigations about the disaggegation of organocuprates by dilution, variable temperatures and the addition of THF showed that the results of the linear chain models of salt-free organocuprates and cyanocuprates shown in Figure 13a, c, and d met the expectations for these systems. In summary, these diffusion NMR investigations of organocuprates in diethyl ether show molecular sizes larger than dimers and an aggregation dependent on steric hindrance, salt effects, and sample concentration. Steric hindrance as well as low concentration decrease the degree of aggregation whereas the presence of salt, especially LiCN increases aggregation. The experimentally determined extent of solvation and the trend of cyanocuprates to form higher aggregates confirm the homodimeric core structure of salt-containing cuprates in diethyl ether.[24]

3.2.5. Aggregate Structures beyond Dimers Influence Reactivity

From the combined investigations described above, a structural model for dialkylcuprates in diethyl ether emerges. The homodimeric core structures are connected by solvent- and salt-bridges and especially LiCN promotes oligomerization, whereas salt-free cuprates and cuprates with LiI show similar aggregation levels only a little higher than homodimers. Now the question arises whether the differences in reactivities of organocuprates are connected with the degree and type of oligomerization in solution.

In diethyl ether, kinetic data for Me_2CuLi•LiI were published by Canisius et al.[223] and Bertz et al.[163] presented relative reactivities from logarithmic reactivity profiles for many organocuprates under various conditions; for example, Me_2CuLi•LiI•2THF, Me_2CuLi•LiI, and Me_2CuLi•LiCN at 0.1 M. Among these three cuprates Me_2CuLi•LiI•2THF was reported to be the most reactive one, closely followed by Me_2CuLi•LiI, and Me_2CuLi•LiCN was by far the least reactive cuprate. A combination with our oligomerization trends of these three organocuprates measured at concentrations between 0.5 and 0.8 M suggested the homodimer as reactive species. However, the oligomerization equilibria of copper complexes in solution are especially very sensitive to different experimental conditions such as varying temperatures, concentrations or solvents, which caused a lot of confusion about the reactivities of cuprates in the literature. Therefore, kinetic studies and NMR structural investigations were performed under identical experimental conditions, to evaluate the influence of oligomerization and of potential disaggregation by THF on the reactivity of organocuprates.[29] The combined results of kinetic data and diffusion experiments are shown in Figure 14.

Surprisingly, different influences of THF on the reactivity and on the aggregate structure are found for Me_2CuLi•LiI and Me_2CuLi•LiCN at various concentrations. For Me_2CuLi•LiI, the addition of 0.25−1.00 equivalents of THF leads to pronounced acceleration effects. In contrast, the reaction rates of Me_2CuLi•LiCN, being remarkably higher in pure diethyl ether, significantly decrease upon addition of THF. This decline of the reaction rates seems to be directly correlated to a disaggregation of the oligomeric structure of Me_2CuLi•LiCN, as shown by the corresponding diffusion experiments (see Figure 14b and d). In contrast, in the case of Me_2CuLi•LiI, the surprising maxima in reactivity are not at all reflected in the diffusion coefficients (see Figure 14a and c). This shows one of the important drawbacks of diffusion experiments. Small structural changes, which do affect the hydrodynamic radius of aggregates only within the error range (ca. ± 5% of the experimental self-diffusion coefficient), can not be detected by diffusion experiments.

In such a situation, ^{1}H, ^{7}Li HOE- and ^{1}H, ^{1}H NOE studies are promising. The nuclear Overhauser effect is very sensitive to small structural changes due to its r^{-6} distance dependence and the cut off distance of ca. 5 Å. In addition, the linear oligomer structure restricts the observed effects to changes within the dimer and its salt bridges. However, the difficulty and the potential of nuclear Overhauser effects in such flexible systems are simultaneously the relative quantification of HOEs and NOEs between different samples and in the absence of evident reference cross signal. For the ^{1}H, ^{1}H NOEs the only fixed distance between the chemically inequivalent CH_2-groups of THF can be used, but the increasing amounts of THF have to be included by normalization. For the ^{1}H, ^{7}Li HOEs the situation is even more difficult because there is no fixed distance at all. Here, a relative calibration is only possible on the basis of the previously gained structural information combined with the results of the diffusion experiments. The distance studies on the homodimeric core also showed for salt-containing cuprates that mainly the lithium ions in the homodimer contribute to the HOE and that the additional lithium ions can be neglected in a first assumption. In addition, the diffusion studies indicated the preservation of the homodimer. Therefore, the HOE between lithium and the methyl-groups of the cuprates could be used for calibration.

Even with calibration methods at hand, again the identification and the visualization of the crucial structural parameter is essential. In Figure 15a, a homodimer connected with one of the possible salt bridges is shown. In case the addition of THF does not affect the basic oligomer structure and only the solvent molecules are exchanged from diethyl

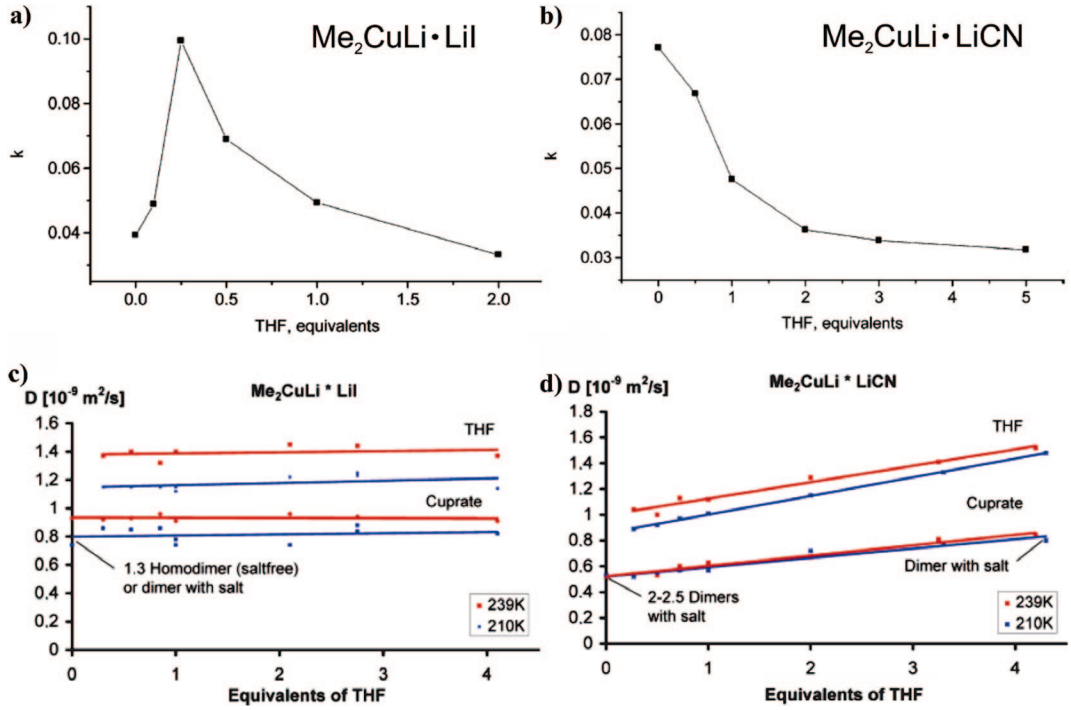

Figure 14. Rate constants of the 1,4 addition of $Me_2CuLi•LiI$ (a) and $Me_2CuLi•LiCN$ (b) to 4,4-dimethylcyclohex-2-enone in pure diethyl ether and in solvent mixtures of diethyl ether and different equivalents of THF; diffusion coefficients of the pure reagents $Me_2CuLi•LiI$ (c) and $Me_2CuLi•LiCN$ (d) under otherwise identical experimental conditions. Reprinted with permission from ref 29. Copyright 2005 American Chemical Society.

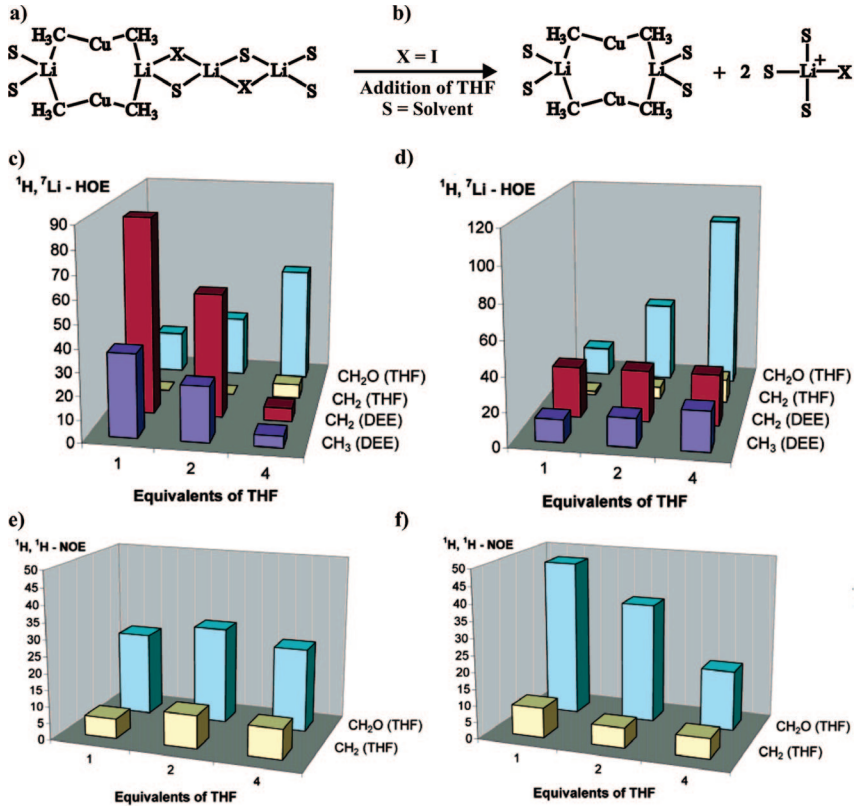

Figure 15. Postulated aggregate structure (a) and disaggregation in the case of $X = I$ (b); bar charts summarizing the ^1H, ^7Li HOE volume integrals of the cross-peaks between lithium and the protons of diethyl ether and THF for $Me_2CuLi•LiI$ (c) and $Me_2CuLi•LiCN$ (d) and bar charts summarizing the ^1H, ^1H NOEs between the methyl groups of the cuprate and the CH_2-groups of THF for $Me_2CuLi•LiI$ (e) and $Me_2CuLi•LiCN$ (f). Reprinted with permission from ref 29. Copyright 2005 American Chemical Society.

ether to THF, a steady increase of the ^1H, ^7Li HOE-signals to THF should be detected with increasing amounts of THF. Simultaneously, the ^1H, ^7Li HOE-signals to diethyl ether should decrease. In fact, this behavior is detected for $Me_2CuLi•LiCN$ (see Figure 15c). However, in the interesting case of $Me_2CuLi•LiI$ the cross-peaks of THF increase in a superproportional manner, while the diethyl ether cross signal volume integrals remain nearly constant. This reveals the

structural change not detectable by diffusion experiments. The diethyl ether molecules are not only replaced by THF, but additional coordination sites are also generated most probably by dissociation of solvated lithium ions as shown in Figure 15a, b. A dissociation of salt units from the cuprate core should additionally cause a reduction of the ^{1}H, ^{1}H NOE between cuprate and THF. This decrease is exactly observed for Me_2CuLi•LiI (see Figure 15f), whereas the NOE intensities remain constant in the structurally stable repetition unit of Me_2CuLi•LiCN (see Figure 15e).

Thus, the structural change in the oligomeric aggregate is elucidated. In Me_2CuLi•LiI small salt units are displaced upon the addition of THF. The reactivity of Me_2CuLi•LiI seems to be fine-tuned by certain amounts of salt or THF influencing the Lewis acidity of the Li^+ cations. In striking contrast, Me_2CuLi•LiCN is disaggregated from short oligomers into dimers by THF without structural change in its core structure. The LiCN remains attached, which is additionally confirmed via ^{1}H, ^{13}C HOE contacts to the CN^- group (see Figure 11). This indicates that the oligomeric structure of cyano dialkylcuprates and/or the Lewis acidity of Li^+ gained by this oligomeric structure influence the reactivity of LiCN-containing cuprates rather than the presence of single LiCN units.

3.3. Diorganocuprate Intermediates

3.3.1. Introduction

Besides NMR, there are other valuable methods providing experimental information about the structures of organocuprates, such as X-ray diffraction methods, EXAFS, XANES, mass spectrometry, and infrared spectroscopy. However, for studying the mechanism of copper mediated reactions in terms of structure elucidation of reaction intermediates, NMR spectroscopy at low temperatures in combination with rapid-injection methods is by far the most promising method. When discussing the potential of NMR for investigating reaction intermediates, it is very important to keep in mind that in principle, transition states can not be studied using NMR and minor conformations are often not accessible either. But the investigation of the structures of reagents and intermediates in solution is an essential prerequisite for choosing the ideal starting structures for theoretical calculations, which in turn should be capable to reveal transition state structures.

Until now it has been possible to observe a couple of intermediate π-complexes in the reaction pathways of 1,4-,[206,224–232] 1,6-,[233–235] and 1,8-addition reactions of cuprates. Very recently even a Cu(III) intermediate[236] was detected in a 1,4-addition reaction.[236] Shortly after the finding of this first Cu(III) intermediate other Cu(III) intermediates of substitution reactions were discovered.[236–238] In principle, the NMR methodical possibilities to gain structural information about intermediates are identical to the methods described above for the reagents in solution. However, the finding and stabilization of intermediates usually demand knowledge about low reactivities or slowly reacting systems as well as great skills and experience in low temperature preparations and NMR detection of minor species. In the following, both organocuprate π-complexes and the Cu(III) intermediates will be described.

3.3.2. Organocuprate π-Complexes

The formation of organocuprate π-complexes as intermediates in all kinds of addition reactions and also in substitution reactions with allylic substrates is proposed in numerous theoretical studies.[22,28,239–246] For example, a dimethylcuprate enone π-complex is schematically shown in Figure 12. For the detection of intermediate organocuprate π-complexes NMR spectroscopically with the utmost probability, slowly reacting systems were chosen in the beginning, for example, THF as solvent, conjugated carbonyl compounds with reduced reactivity such as cinnamates,[226–228,231] bulky enones as substrates[247] (e.g., 10-methyl-$\Delta^{1,9}$-2-octalone[224]) or sterically hindered cuprates (e.g., t-Bu_2CuLi•LiCN[233,234] or t-BuCu(CN)Li[229]). In contrast to these demanding stabilization procedures for dialkylcuprates, for chiral amidocuprates a monomeric π-complex with cyclohexenone could be directly observed in diethyl ether, due to the different lithium coordinating properties of amidocuprates (see section 3.4).[235]

In the beginning, the structural assignment of lithium carbonyl complexes and cuprate-enone π-complexes was solely based on the differences in the ^{13}C chemical shifts of the enone observed before and after adding cuprate. The coordination of a cuprate with the π-system induces large upfield shifts of the resonances of carbons involved in the C−C double bond, whereas an interaction of a lithium ion of the cuprate cluster with an oxygen atom causes small downfield shifts of the carbonyl resonances.[224,226–228,231,233,248] These chemical shift differences are exemplarily shown on a cuprate-enyne π-complex in Figure 16.[225] In these NMR studies ^{13}C labeling on selected positions in the enones was often used to verify the assignment after complexation.

Additional information about the bonding situation in these π-complexes was gained by ^{13}C−^{13}C and ^{1}H−^{13}C coupling constants.[234] For example INADEQUATE[249–256] experiments were used to detect $^1J_{C,C}$ coupling constants before and after complexation with cuprates, again with the aid of ^{13}C labeling at selected positions of the enones or the ynoates (see Figure 17). The exclusive reduction of the C−C coupling constant within the former double bond shows that the triple bond does not interact with the cuprate and the reduction of this structurally important $^1J_{C,C}$ to 49−54 Hz reveals a hybridization similar to a single bond connecting two carbon atoms with sp^2 hybridization.[234]

In addition, structural information about the cuprate part in these π-complexes can be derived from scalar coupling constants and NOEs between the cuprate moiety and the substrate. In these π-complexes, the two cuprate substituents are differently oriented in relation to the substrate and give rise to separate signals with individual coupling constants and NOEs at low temperatures. Thus, for example, $^2J_{C,C}$ coupling constants of 12 Hz from one of the cuprate methyl groups to one of the enyne carbons were detected[225,234] (see Figure 18a) as well as a reduction of the $^2J_{C,C}$ coupling constants within the cuprate unit from 21 to 4 Hz.[225] Both experimental facts indicate a non linear arrangement of the cuprate methyl groups within the π-complexes. At the same time a nearly linear alignment of the two carbons can be stated, which show the 12 Hz scalar coupling constant across copper. The resulting structure and the orientation of the cuprate unit within these π-complexes was confirmed by NOESY and ROESY spectra. Recent π-complex investigations on substituted enones in diethyl ether also showed the π-complex structure displayed in Figure 18b to be a general feature.[257]

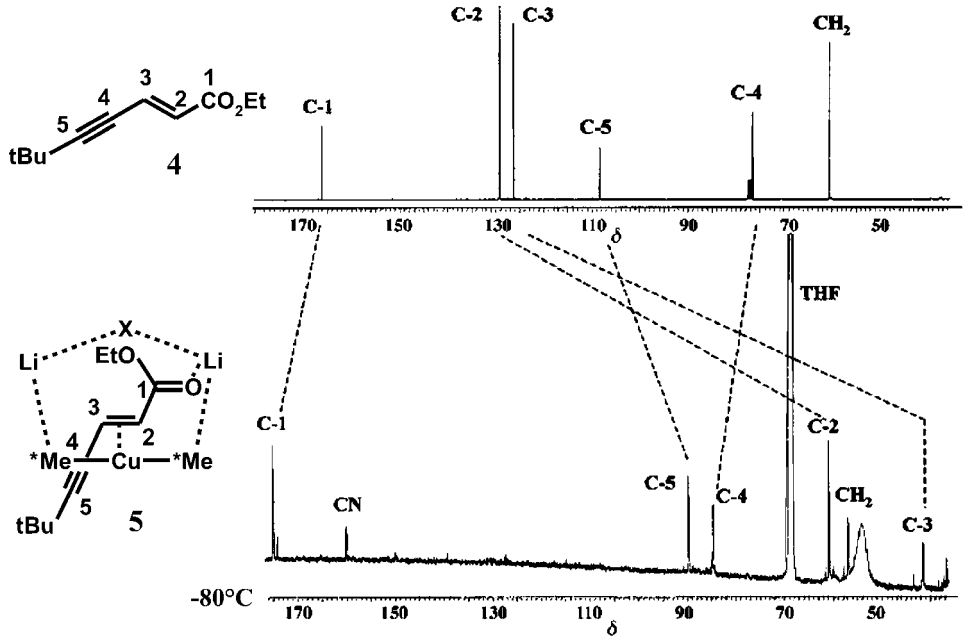

Figure 16. ^{13}C NMR spectra of the 2-en-4ynoate **4** and its cuprate-enyne π-complex **5** show typical ^{13}C chemical shift changes upon carbonyl complexation and π-complex formation. Reprinted with permission from ref 225. Copyright 2001 Wiley VCH.

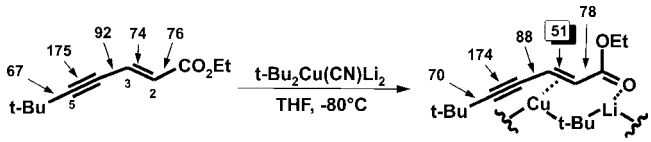

Figure 17. Comparison of the $^1J_{C,C}$ coupling constants of the ynoate before and after formation of the π-complex show the exclusive coordination of the cuprate to the former double bond. Reprinted with permission from ref 234. Copyright 1994 American Chemical Society.

C,C Coupling constants	
$J_{2,3}$	53 Hz
$J_{a,b}$	≤ 4 Hz
$J_{2,a}$	0 Hz
$J_{2,b}$	~ 0 Hz
$J_{3,a}$	12 Hz
$J_{3,b}$	0 Hz

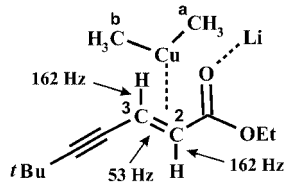

Figure 18. Typical C−C coupling constants within a cuprate enone π-complex indicating a kink in the cuprate unit attached to the double bond. The orientation of the cuprate unit is validated by NOESY cross peaks. Reprinted with permission from ref. 225 Copyright 2001 Wiley VCH.

Later on, the application of rapid-injection techniques[207,208] also allowed the observation of π-complexes formed by the prototypical Gilman reagents Me_2CuLi•LiI and Me_2CuLi•LiCN and the sterically unhindered enone 2-cyclohexenone as already described in section 3.2.3 (see Figure 12).[121] All of the NMR-studies discussed so far used THF as solvent at temperatures of at least 173 K. This choice of the experimental conditions has two great advantages. First, the reaction rate of addition reactions is significantly lower in THF (see section 3.2.2) and second, the structural investigations are not complicated by the formation of higher aggregates in solution because SSIPs are preferred in THF. A well directed substitution pattern of enones in combination with selected solvent mixtures enabled structural investigations of the structural features of diastereomeric and supramolecular π-complexes in diethyl ether, too.[257] For Me_2CuLi or Me_2CuLi•LiI and 10-methyl-$\Delta^{1,9}$-2-octalone in diethyl ether, the existence of two intermediate π-complexes on both sides of the double bond is detected for the first time. The formation of the major species, the β-face complex, is supported by a conformational change of the enone minimizing its steric hindrance with the cuprate moieties.[257] These results give the first experimental insight into the intermediate structures leading to the high diastereoselectivities observed in 1,4 additions to chiral enones. Furthermore, the general patterns observed for π-complexes in diethyl ether show an identical core structure as found in THF. But similarly to the situation of the free reagents, the π-complexes are incorporated into large supramolecular structures mediated by the carbonyl complexing moiety, which is composed of salt and cuprate units.[257] These results show that the supramolecular structures of the π-intermediates are most probably crucial for the diastereoselectivities and the reactivities of organocuprates in 1,4 additions to enones.

3.3.3. Cu(III)-Intermediates

Recently, a true highlight of structure elucidation of copper complexes in solution was published: The observation of the first Cu(III) complexes stabilized in solution.[236–238,258] In the proposed reaction pathways of organocopper reagents, the reductive elimination of Cu(III) intermediates has long been postulated to be the decisive step in typical reactions such as conjugate addition reactions to enones, carbocupration, and S_N2-like reactions of organic halides.[3,167,206,259,260] While these Cu(III) intermediates have been reproduced many times virtually in computational investigations,[22,239,243–246,261–263] it has not been possible to detect them experimentally for more than three decades. Then, within half a year and completely independent from each other the group of Bertz and Ogle and our own group detected several Cu(III) intermediates. Interestingly, the two groups used unequal experimental conditions to stabilize the Cu(III) intermediates, for example, different solvents, enones, alkylhalides and NMR equipments (rapid-injection NMR and conventional low temperature NMR). Despite the theoretically expected instability of Cu(III) complexes,[264] in both cases some

Scheme 1. Two Routes to the First Cu(III) Intermediate, Which Was Observed in the Reaction Pathway of a Conjugate Addition Reaction[a]

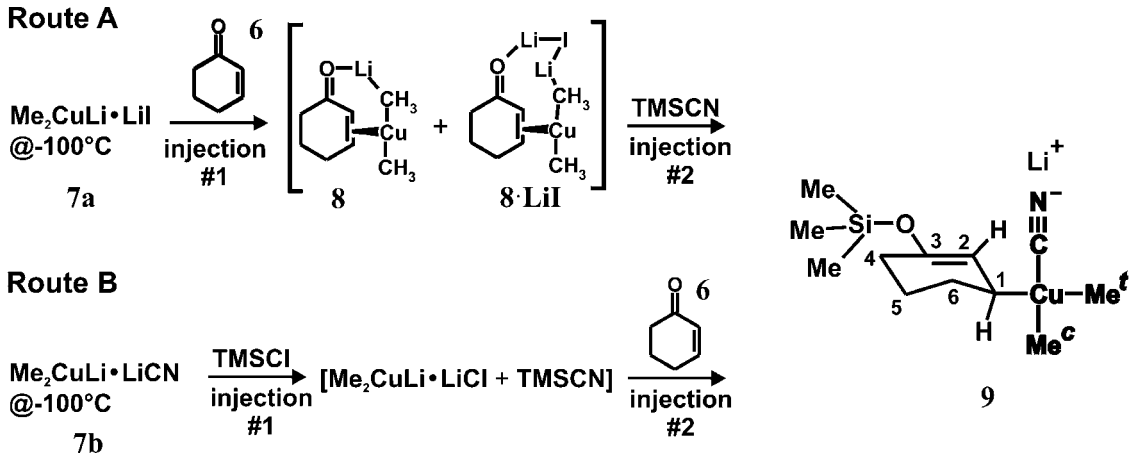

[a] Reprinted with permission from ref 236. Copyright 2007 American Chemical Society.

Table 2. Comparison of ^{13}C NMR (^{1}H NMR) Chemical Shifts for Cuprates, Cu(I) π-Complexes, and Cu(III) Intermediates[a]

group	6	7a	7b	8	8-LiI	8-LiCN	9
CH_3 (CH_3^t)[b]		−9.12 (−1.40)	−9.04 (−1.35)	−5.02 (−1.12)	−5.56 (−1.16)	−5.76 (−1.15)	12.43 (0.05)
CH_3 (CH_3^c)[b]		−9.12 (−1.40)	−9.04 (−1.35)	−0.57 (−0.10)	−1.85 (−0.24)	−2.14 (−0.21)	25.31 (0.53)
CN			158.89			159.20	153.78
C_1 (C_3)[b]	198.65			194.75	193.34	193[c]	144.73
C_2−H (C_2−H)[b]	130.12 (5.90)			77.45 (3.77)	75.82 (3.68)	75.27 (3.71)	116.28 (5.02)
C_3−H (C_1−H)[b]	151.65 (7.08)			61.50 (3.26)	61.50 (3.19)	61.51 (3.17)	39.68 (2.74)

[a] Parts per million from TMS. Values for C atoms attached to Cu are in boldface. Reprinted with permission from ref 236. Copyright 2007 American Chemical Society. [b] Labeling for **9**. Note that C_1 of **6** becomes C_3 of **9** and C_3 of **6** becomes C_1 of **9**. [c] Shift could not be measured accurately, owing to broadening.

of the Cu(III) intermediates were found to be stable for days under the experimental conditions applied. This enabled detailed NMR analyses of the structures of these synthetically very important Cu(III) species and hopefully it will soon be possible to explain the high stereoselectivities of organocopper reactions based on the structural behavior of these Cu(III) complexes.

The first Cu(III) intermediate was stabilized in a conjugate addition reaction by the group around Bertz and Ogle[236] as a further development of their rapid-injection NMR technique of the cuprate enone π-complexes described above.[121] By adding trimethylsilyl cyanide (TMSCN) or trimethylsilyl chloride (TMSCl) to 2-cyclohexenone as substrate and Me_2CuLi•LiI or Me_2CuLi•LiCN as Gilman cuprate, a Cu(III) intermediate was stabilized for the first time (see Scheme 1). The chemical shifts observed for this Cu(III) complex differ significantly from those observed in cuprates or cuprate π-complexes (see Table 2). Especially the ^{13}C chemical shifts of the methyl groups directly bound to copper shown down field shifts $\Delta\delta$ of up to 27.5 ppm (see Table 2). With the aid of ^{13}C labeled methyl groups and cyanide, $^{2}J_{C,C}$ scalar coupling constants across Cu(III) were detected to be 35.4 and 38.1 Hz for the trans arrangement and 2.9 and 5.4 Hz for the cis arrangement. These scalar coupling patterns and the observed chemical shifts were consistent with a concomitant theoretical investigation of a square planar Cu(III) complex.[261]

Later on, we stabilized the first Cu(III) intermediate of a substitution reaction of Gilman cuprates with alkyl halides in diethyl ether.[238] This was done even without the use of a rapid-injection unit by conventional low temperature NMR. Interestingly, our study started similar to that of Bertz and Ogle, with the stabilization of intermediate π-complexes in

Scheme 2. Two Routes to Obtain Cu(III) Intermediates of Substitution Reactions in Diethyl Ether[a]

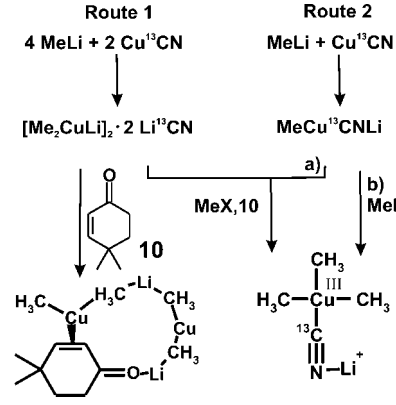

[a] Addition of 4,4-dimethylcyclohexenone to Me_2CuLi•LiCN yields the π-complex as main product. MeX represents traces of methyl halides in commercially available MeLi solutions (see text). Reprinted with permission from ref 238. Copyright 2007 American Chemical Society.

the conjugate addition reactions of Gilman cuprates to enones. However, the different solvents employed in these two independent studies produce significant differences. As discussed above, the SSIPs as main species in THF slow down the reaction rates in conjugate addition reactions. To detect intermediate species in diethyl ether, the reaction rate has to be slowed down by other methods. Therefore, we used an alkyl substituted enone,[265] 4,4-dimethylcyclohexenone, and prepared Me_2CuLi•LiCN with isotopically labeled $Cu^{13}CN$ to enhance sensitivity (see Scheme 2 Route 1).

Surprisingly, in addition to the expected π-complex, very small traces of a copper species with two chemically inequivalent methyl groups and one cyanide attached were

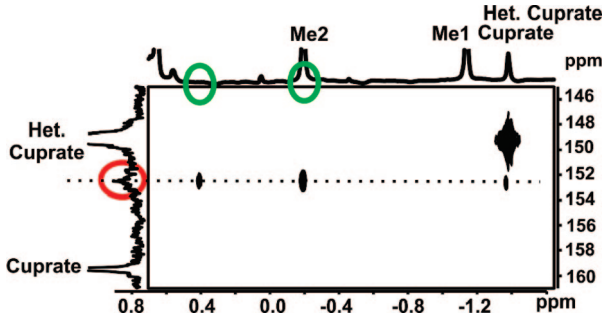

Figure 19. One-dimensional ^{1}H-spectrum of a cuprate enone mixture according to Route 1 in Scheme 2 shows only the two methyl groups of the Cu(I) π-complex (Me1, Me2) and the cuprate reagent. The green circles indicated the positions of the methyl groups in the Cu(III) complex. Only in the cyanide section of a ^{1}H, ^{13}C HMBC spectrum is the new Cu(III) intermediate detected.

observed in a ^{1}H,^{13}C HMBC spectrum (see Figure 19). The amount of this new copper species was so small that no signal was detected in the one-dimensional ^{1}H spectrum due to limitations in the dynamic range of the receiver (see Figure 19). Only the tremendous enhancement of the methyl group signals, connected via $^{3}J_{H,C}$ scalar couplings to the ^{13}C labeled cyanide group, allowed its observation in the HMBC spectrum. Later on, it became evident that the observed intermediate originated from traces of methyl halide in commercially available MeLi solutions and that reduced amounts of Cu(III) intermediate of this S_N2 like substitution reaction can also be obtained directly without enone (see Route 2 in Scheme 2).[238]

By changing the experimental conditions (Scheme 2 Route 2a) the π-complex was completely suppressed and the amount of the new copper species considerably increased. This allowed the in-depth investigation of this new Cu(III) intermediate with ^{1}H, ^{13}C HMBC experiments. As shown in Figure 20, all cross signals expected for a square planar Me_3Cu(III)CN complex with two chemically inequivalent kinds of methyl groups were observed in the ^{1}H,^{13}C HMBC spectrum (for details see the caption of Figure 20 and ref 238).

In the Cu(III) intermediate of the conjugate addition reaction (see above) the postulation of square planar coordination sphere on copper was based on precedent[266,267] and on high level theoretical calculations.[261] In contrast, if exclusively methyl groups are used as alkyl substituents, the square planar coordination of the Cu(III) intermediate is directly evident from the proton spectrum and the HMBC spectrum discussed above. In addition, the square planar coordination is in perfect agreement with crystal field theory, because square planar d^8 Cu(III) complexes are expected to be diamagnetic resulting in sharp NMR signals and chemical shifts close to those of organic compounds. This is also in agreement with the finding that most of the known crystal structures of Cu(III) compounds show a square planar environment with different degrees of distortion around Cu(III).[268] In contrast, tetrahedral d^8 Cu(III) complexes are expected to be paramagnetic, due to two unpaired electrons within the three t_{2g} orbitals resulting in very broad signals and extreme low field shifts of the protons close to the paramagnetic center.

Simultaneously to the detection of Cu(III) intermediates in substitution reactions in our laboratory, Bertz and Ogle used organic halides to detect Cu(III) species with rapid-injection NMR (see Figure 21).[258] Interestingly, the Cu(III)

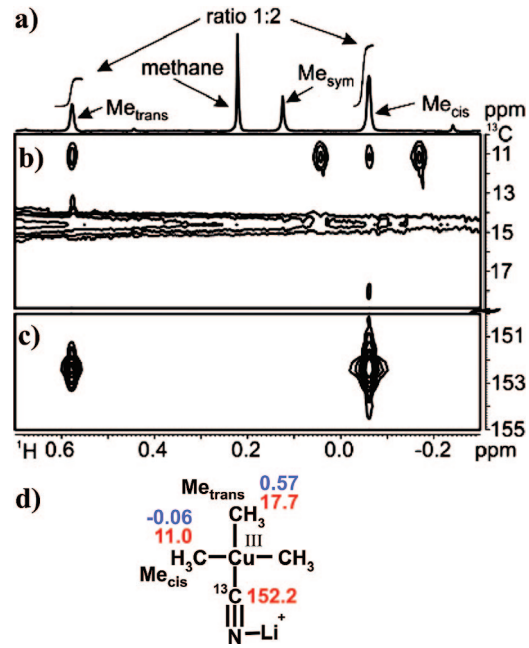

Figure 20. Selected high field sections of a 1D ^{1}H spectrum (a) and a ^{1}H,^{13}C HMBC spectrum (b, c) show all cross-peaks expected for the square planar Cu(III) intermediate (d) with ^{13}C (red) and ^{1}H (blue) chemical shifts. The proton spectrum (a) shows a 1:2 ratio of Me$_{trans}$ and Me$_{cis}$ as well as signals of methane and a species Me$_{sym;}$ the methyl section (b) and the cyanide section (c) of the HMBC spectrum show that two chemically equivalent methyl groups together with a third methyl group and a cyanide group are attached to copper. Reprinted with permission from ref 238. Copyright 2007 American Chemical Society.

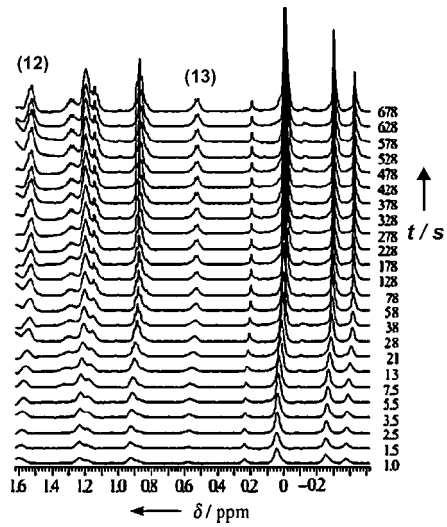

Figure 21. Formation of Cu(III) intermediates in substitution reactions using rapid-injection NMR and ^{1}H NMR spectra obtained from the rapid-injection treatment of Me_2CuLi•LiCN (**11**) with EtI. Signals of Cu-bound methylene groups are labeled **12** for $Me_2EtCuCN$ and **13** for Me_3EtCu. Reprinted with permission from ref 258. Copyright 2007 Wiley VCH.

intermediate with three methyl groups as alkyl substituents on copper could not be detected in THF, not even with the aid of rapid-injection NMR. However, by the use of larger alkyl halides for the substitution reaction, five different Me_2EtCuX species were observed.[258] In these experiments the first tetraalkyl Cu(III) complex, Me_3EtCu, was unambiguously assigned and found to be even more stable than Me_2EtCuX. Furthermore, several neutral RR'_2Cu(III)L complexes were detected, which had been prepared

from $Me_2CuLi•LiI$ and alkyl halides in the presence of strongly electron donating ligands (e.g., PBu_3, $P(OMe)_3$, pyridine).[237]

An interesting aspect of these four Cu(III) studies are the different methods for the stabilization of the Cu(III) intermediates. The study on the conjugate addition intermediate was carried out in THF, which is known to reduce the reaction rates by supporting the formation of solvent separated ion pairs. Even so, the conjugate addition Cu(III) intermediate had to be trapped with trimethylsilyl cyanide or trimethylsilyl chloride (see Scheme 1). In contrast, the substitution reactions are known to proceed faster in THF than in diethyl ether. But in THF, only ethyliodide, i.e. an alkyl substituent slightly larger than methyl, was sufficient to obtain stable Cu(III) intermediates. The fact, that Me_3CuCN intermediates were detected in diethyl ether but not in THF, is in good agreement with the proposed solvents reactivity correlation of substitution reactions. These observations raise the question, whether the Cu(III) intermediates appearing in substitution reactions are in general more stable than those in conjugate additions.

In summary, the described structural investigations of cuprate reagents and intermediates in solution show impressively that it is possible to investigate even highly symmetrical aggregate structures of organocopper reagents or instable intermediate complexes in detail by means of advanced NMR methods. Combined information from scalar coupling constants and sophisticated NOE-, HOE-, and diffusion experiments are advantageous for the structure determination of aggregates. Rapid-injection NMR and/or elaborate preparative stabilization methods combined with low temperature NMR allow the detection of decisive intermediate structures.

3.3.4. Kinetic Isotope Effects

Interestingly, NMR spectroscopy in combination with theoretical calculations was also used to identify the rate determining step of copper promoted reactions.[269–272] Singleton and co-workers introduced a powerful NMR spectroscopic technique for measuring ^2H and ^{13}C kinetic isotope effects at natural isotopic abundance, which is based on the determination of the relative proportion of the isotope in question within the product (low conversion) or the substrate (high conversion) under carefully controlled conditions.[273] With the aid of this method, the formation of the C−C bond, that is, the reductive elimination, was found to be rate-determining in 1,4- as well as in 1,6-addition reactions.[242,270] On the other hand, in the case of substitution reactions with alkenyl bromides the C−Br bond cleavage was found to be rate determining.[272] Furthermore, with kinetic isotope effects, mechanistic differences were revealed between the cuprate chemistry described here and Cu catalyzed 1,4-addition reactions with dialkylzinc.[271]

3.4. Heteroleptic Lithium Amidocuprates

Lithium organo-amidocuprates differ from homocuprates, $[R_2CuLi]$, by replacement of one of the reactive organo groups with a nontransferable amido group. This structural modification changes essentially the parameters accessible to NMR spectroscopy. First, the exchange rate of structurally inequivalent lithium ions is significantly reduced to the slow exchange limit on the NMR time scale. This does not only allow the observation of several separated ^7Li NMR signals,

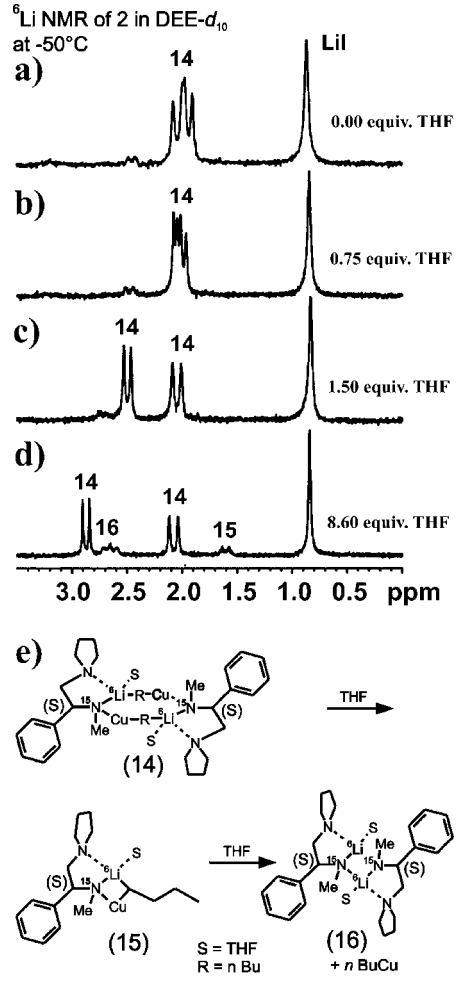

Figure 22. ^6Li NMR spectra of **14** at 223 K in (a) diethyl ether-d^{10}, (b) diethyl ether-d^{10} with 0.75 equiv of THF-d^8, (c) diethylether-d^{10} with 1.5 equiv of THF-d^8; (d and e) schematic representation of the dimer in diethylether and its dissociation upon addition of increasing amounts of THF. Reprinted with permission from ref 144. Copyright 2000 American Chemical Society.

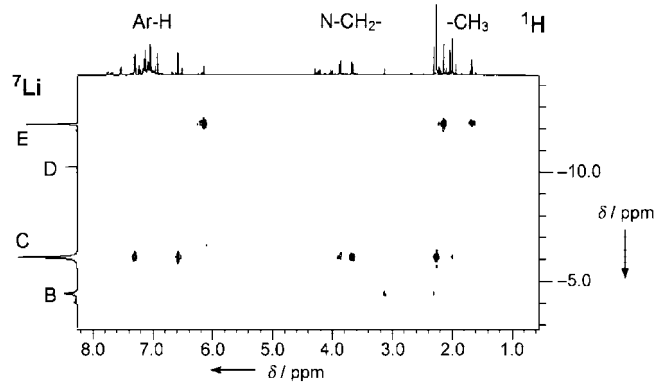

Figure 23. ^1H, ^7Li HOESY NMR spectrum of $[Cu_2Li_2Mes_2(N(CH_2Ph)_2)_2]$ in toluene-d^8 shows several separated lithium signals and various HOE cross-peaks allowing for a more classical NMR approach in the structure elucidation of amidocuprates. Reprinted with permission from ref 280. Copyright 2007 Wiley VCH.

but also the quantitative detection of $^nJ_{Li,N}$ scalar coupling constants in ^{15}N labeled samples (see Figure 22a−d). As already mentioned in section 3.1 the detection of these scalar couplings to lithium allows for a structure elucidation process comparable to that of organolithium compounds or lithium complexes with chiral amine ligands, in which scalar

Scheme 3. Predicted Schlenk-Like Equilibrium for the Lithium Heterocuprate $[Cu_2Li_2Mes_2(N(R)_2)_2]$ in Toluene (R = CH_2Ph)[a]

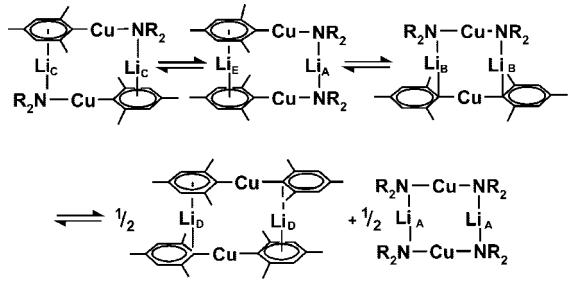

[a] Reprinted with permission from ref 280. Copyright 2007 Wiley VCH.

couplings and nuclear Overhauser effects are widely used to determine their aggregation and structure in solution.[146–154]

The previously proposed[274–276] dimer structure of amidocuprates in diethyl ether was verified[144] by using a sophisticated interpretation of the $J_{Li,N}$ scalar coupling constants and multiplicity patterns[277–279] combined with 1D and 2D experiments based on ^1H, ^6Li, ^{15}N, and ^{13}C NMR heterocorrelation spectroscopies. In addition, a decomposition of the amidocuprate **14** into **15**, and finally into **16** and even into non complexed *n*-BuCu was structurally proven with the same spectroscopic techniques (see Figure 22e).

For $[Cu_2Li_2Mes_2(N(CH_2Ph)_2)_2]$, the detection of several separated Li signals in this amidocuprate allowed the identification of a mixture of structural isomers that is present in toluene solution due to a Schlenk-like equilibrium (see Scheme 3)[280] This was achieved with the aid of indirectly detected ^1H, ^7Li HOESY experiments[281,282] (see Figure 23) and the interpretation of lithium chemical shift data.[280,283,284] The separated lithium signals and the well distributed proton signals of the amidocuprate allow the detection of a number of HOE cross-peaks for each structural isomer and in the absence of significant exchange contributions. This enables a more classical structure elucidation approach, which is not applicable to homocuprates (see section 3.2).

4. Catalytic and Precatalytic Copper Complexes with Chiral Ligands

4.1. Introduction

In the wide field of catalytic copper complexes (comprised of copper salts and chiral ligands), very little was known about the structures of the precatalytic copper complexes or the catalytically active species in solution for a long time, especially in case of several metal centers being present.[3] Only a few recent publications provide the first insight into the structural arrangements of such copper complexes in solution, which are described in detail in this section.

In the majority of copper complexes with chiral ligands, the structural parameters accessible to NMR are even more limited than in the case of organocuprates. Especially, in complexes with P-, N-, or S-donor ligands and symmetries deviating from a rigorous tetrahedral coordination on copper, no scalar coupling constants across copper are usually detectable. For the structure elucidation process this means that the number of ligands attached to copper can not be determined by scalar coupling patterns, and the monomer structure has to be defined by other means. In the following, possible structure elucidation pathways for such copper complexes will be explained on the basis of selected examples. However, this list is not exhaustive.

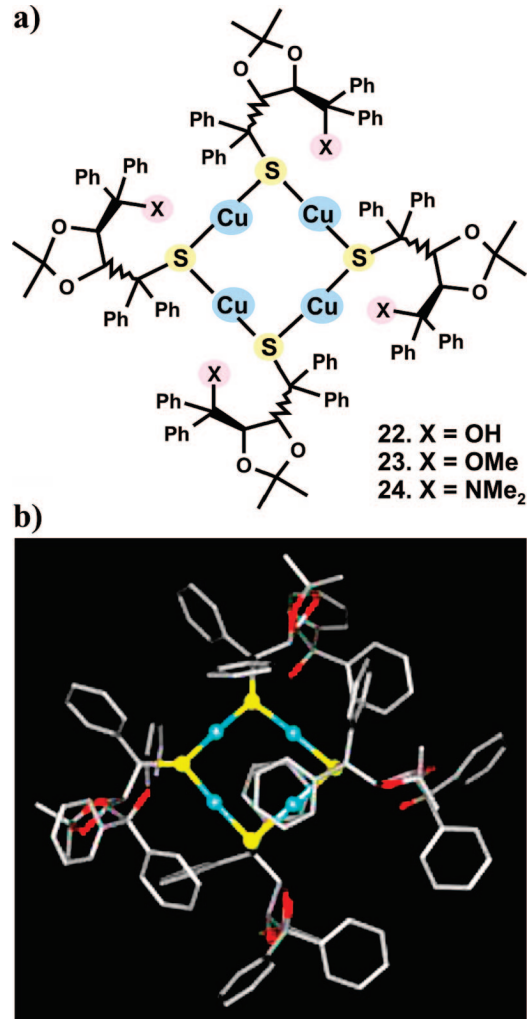

Figure 24. Schematic representation (a) and structure of the tetranuclear Cu complex **22** based on X-ray diffraction data (b). The H atoms have been omitted for clarity; O atoms are indicated in red, S atoms in yellow, and Cu atoms in blue. Reprinted with permission from ref 285. Copyright 2000 Wiley VCH.

4.2. Thiolate Copper Complexes

One intriguing example of tetranuclear copper thiolate complexes was published by the groups of Seebach and Pregosin.[285] In enantioselective 1,4-addition reactions of Grignard reagents to enones, an unexpected selectivity inversion was observed using CuCl and the thiols **17** - **19** (see Scheme 4).[286] Modest positive nonlinear effects suggested that more than one ligand (and perhaps several metals) might be involved in the catalysis.[287–289]

Because higher molecular weight copper thiolates used in catalysis are isolable in the solid state,[290] the possible aggregation levels of these complexes in solution were considered. The crystal structure of **22** shows a tetranuclear Cu complex, in which the TADDOL-derived[291] thiol surprisingly acts as a monodentate and not as a bidentate ligand for CuI (see Figure 24). In an attempt to prepare models related to the copper chemistry in the copper catalyzed 1,4-addition reactions of Grignard reagents (see Scheme 4), the complexes **22**−**24** (Figure 24) were allowed to react with an excess of *tert*-butylisocyanide in THF-d^8 which was supposed to model an additional donor ligand. Though the

Scheme 4. (a) Thiol-TADDOL ligands 17−19 and (b) Copper-Catalyzed Conjugate Addition: e.r. 92:8 (with 17), e.r. 8:92 (with 18 or 19)[a]

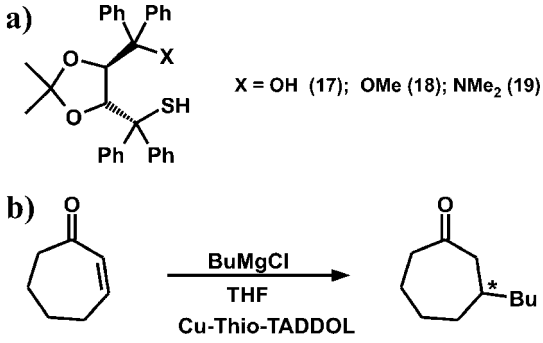

[a] Reprinted with permission from ref 285. Copyright 2000 Wiley VCH.

Scheme 5. Fragment Showing the Composition of the Isocyanide Complexes 25−27[a]

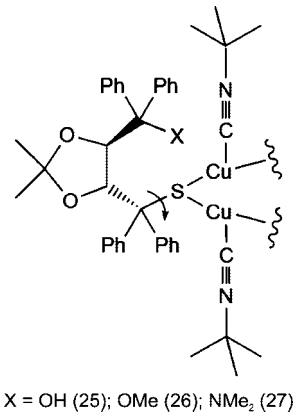

X = OH (25); OMe (26); NMe_2 (27)

[a] ^{1}H, ^{1}H-NOESY spectra of **25**−**27** reveal that **25** adopts a different conformation in the tetranuclear copper complex compared to **26** and **27**. This conformational change is indicated by the arrow showing the possible rotation around the C−S bond. Reprinted with permission from ref 285. Copyright 2000 Wiley VCH.

resulting isocyanide complexes **25**−**27** (see Scheme 5) show exchange of the isocyanide ligands in solution, they are suitable for NMR investigations. With the aid of NMR diffusion data for the ligands **17** and **18**, which exist as hydrogen-bonded dimers or monomers in solution, the hydrodynamic radii of the monomer units were defined. The subsequent ^{1}H NMR diffusion measurements on **25**−**27** revealed that these complexes are tetranuclear species in solution, too and that **22**−**24** do not degrade into mononuclear species in the presence of additional donor ligands. Despite the exchange behavior of the isocyanide ligands in **25**−**27**, in ^{1}H, ^{1}H NOESY experiments, a variety of contacts between the complexed thiolate ligands and the *tert*-butyl group of the isocyanide were detected. These cross-peaks suggest a different structure for **25** relative to **26** and **27** (see Scheme 5). The observed structural deviations create different chiral environments around the copper atom and may be the source of the observed stereochemical inversion noted above. Thus, the accordance of results obtained from solid state structure analysis and from NMR diffusion data as well as chemical shift analyses made it possible to build up a structural model of this tetranuclear Cu complex in solution. In addition to that, NOESY data from interactions between the extensive ligand structure and an additional dummy ligand as structural sensor allowed a structure selectivity correlation of these precatalytic copper complexes.

Scheme 6. Copper Catalyzed Enantioselective 1,4-Addition Reaction of Et_2Zn to Enones with Selected Phosphoramidite Ligands As Representatives for the Binaphthol and Biphenol Ligands Developed in the Groups of Feringa[295] and Alexakis[294a]

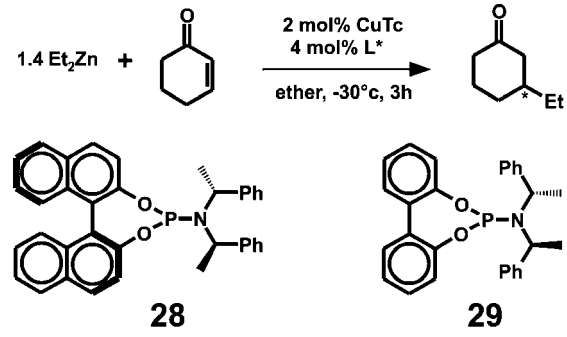

[a] Reprinted with permission from ref 292. Copyright 2000 Wiley VCH.

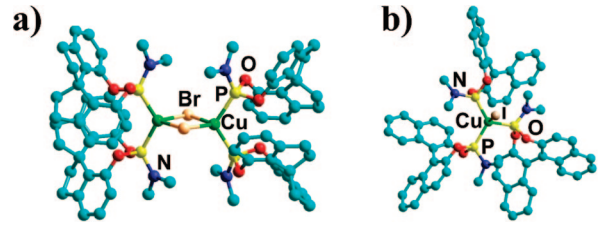

Figure 25. Known crystal structures of phosphoramidite copper complexes; (a) [CuBr(O,O′-(*R*)-(1,1′-Spirobiindane-7,7′-diyl)-*N*,*N*-dimethylphosphoramidite)$_2$]$_2$,[297] (b) CuI(O,O′-(*S*)-(1,1′-Dinaphthyl-2,2′-diyl) -*N*,*N*-dimethylphosphoramidite)$_3$.[296] Reprinted with permission from ref 292. Copyright 2000 Wiley VCH.

4.3. Phosphoramidite Copper Complexes

Another recent example for NMR structure elucidation[292] of precatalytic copper complexes is the breakthrough system for enantioselective 1,4-addition reactions to enones, using phosphoramidite ligands for copper catalyzed dialkylzinc additions (see Scheme 6).[1,293−295] Two published crystal structures of copper complexes with phosphoramidite ligands yielding only moderate enantioselectivities[296,297] offered potential structural models with tetrahedral coordination on copper (see Figure 25). However, these arrangements are quite implausible for ligand accelerated catalyzes.[298] Furthermore, the ^{31}P spectra of these phosphoramidite copper complexes show complicated and broad signals caused by a mixture of several complex species in toluene and THF (see Figure 26a). Thus, the first key step for structure elucidation in solution was to find experimental conditions, which are highly successful in synthetic applications and simultaneously stabilize only one kind of complex in solution. For phosphoramidite copper complexes, the solution to this problem was CD_2Cl_2 or $CDCl_3$ as solvent. In these two solvents two key complexes (named C1 and C2) can be identified by using different copper salt to ligand ratios (see Figure 26a and b). By systematical variation of the ratios of copper salt to ligand in $CDCl_3$, the stoichiometric composition of the crucial precatalytic complex C2 was identified in ^{31}P spectra to be 1.5 ligand per copper (see Figure 26c).

The subsequent determination of the aggregate size is the second challenge in this system. Scalar couplings across copper are not detectable and the transversal relaxation time of the ^{31}P signals is too short to allow diffusion experiments by ^{31}P NMR spectroscopy, not even with special equipment applying stronger gradients. In addition, the ^{1}H signals of the free ligand and the complexes C2 and C1 overlap so

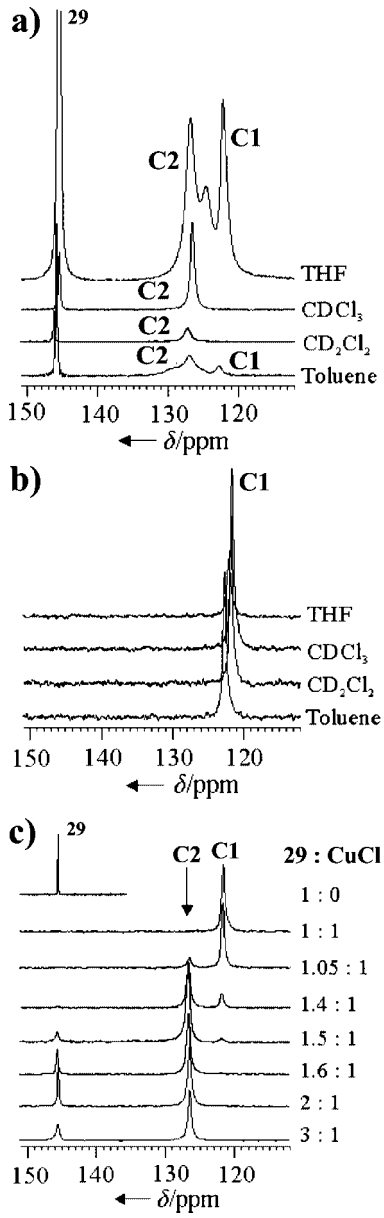

Figure 26. ^{31}P NMR spectra of the complexes formed by **29** and CuCl at a ratio of 2:1 (a) and 1:1 (b) in different solvents show two key complexes (C1 and C2); (c) ^{31}P NMR spectra of **29** and mixtures of **29** and CuCl at varying ratios in $CDCl_3$ reveal the stoichiometric composition of C2. Reprinted with permission from ref 292. Copyright 2000 Wiley VCH.

severely that routine ^{1}H diffusion measurements would lead to unreliable diffusion coefficients of C2 due to nonestimable exchange contributions of the free ligand or C1. The solution for this second problem was to take advantage of the effects of dynamic NMR at 220 K, a temperature close to synthetic applications. The activation barriers for internal dynamic processes within the free ligand and the complexes, especially C2, differ sufficiently to cause different line widths of the methine signals (see Figure 27). As a result, the quite longish convection compensating pulse sequence of Müller and Jerschow acts as immanent T_2-filter for the very broad methine signals of the free ligand and C1, which allows the exclusive detection of contributions from C2.

The resulting diffusion coefficients of C2 in combination with the determined stoichiometry of the complex and known stereochemistries of typical Cu(I) complexes,[21,299,300] allowed the identification of a binuclear copper complex with a mixed trigonal/tetrahedral stereochemistry (see Figure 28a). This new structural motive for catalytically active copper complexes allows a structural explanation of the known synthetic optimization procedures and offers the basis for the design of new improved catalysts.[292] Later on, a screening with four Cu(I) salts and three phosphoramidite ligands revealed that the binuclear complex shown in Figure 28a is a basic structural motif of precatalytic Cu(I) complexes with phosphoramidite ligands affording highly stereoselective reactions.[301] Higher coordination numbers and higher aggregation levels were observed for ligands with smaller amine moieties leading to reduced *ee* values. Interestingly, the fragments observed in ESI mass spectra show a striking correlation with the structures observed in solution, by revealing the maximum number of ligands attached to copper.[301] The existence of the binuclear copper complex with the mixed coordination on the two copper atoms was additionally confirmed by low temperature NMR measurements, because the expected 2:1 pattern was found in the ^{31}P spectra. As additional low temperature species small contributions of a binuclear complex with four ligands were observed, which is tetrahedral coordinated on both copper atoms (see Figure 28b).[302] Furthermore, with the aid of diffusion experiments and ^{31}P integrals it was for the first time possible to follow the formation of different complex species even in mixtures of copper complexes, whose ^{31}P signals are spectroscopically unresolved due to ligand exchange processes.[302] This temperature dependent interconversion show that in case of structurally flexible and/or coordinatively unsaturated chiral copper complexes one has to act with great caution to infer the complex structures in solution at ambient temperatures from known X-ray structures, because the aggregation tendencies are even more pronounced in the solid state than at low temperatures in solution.

4.4. Ferrocene-Derived Diphosphine Copper Complexes

To date only a few mechanistic studies have been reported on enantioselective copper catalyzed conjugate addition reactions of organozinc reagents[271,292,301–305] or Grignard reagents[285,306] and they have not, as yet, led to a general agreement regarding the rate determining step. Despite that, the current mechanistic view proposes as first step a transmetalation of the organic substituent from the organometallic compound to the copper. For that, experimental evidence from NMR chemical shifts exists in two cases.[306,307] The recent extensive spectroscopic and mechanistic studies on copper catalyzed conjugate addition reactions of Grignard reagents are an excellent example of a combination of spectroscopic studies, kinetic analyses, and variation of reaction parameters to provide a mechanistic scheme of this reaction.[306,308,2] From ESI-MS, IR spectroscopy, X-ray crystallography, and electrochemistry studies, the investigated copper complexes with chiral ferrocene-derived diphosphines were found to exist as bromide bridged dinuclear complexes in the solvents used in the conjugate additions (see Scheme 7).[306,308] Based on NMR information from scalar coupling patterns, ^{1}H and ^{31}P chemical shifts, integrals and their changes upon variation of reaction parameters, a dissociation of this binuclear complex as well as a transmetalation upon addition of Grignard reagents was proposed (see Scheme 7).

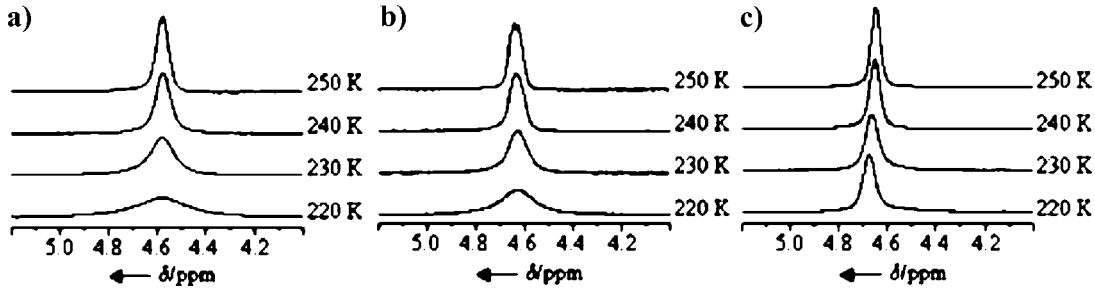

Figure 27. Different line broadening effects of the ^{1}H methine signal in (a) the free ligand 29, (b) C1, and (c) C2 resulting from temperature shifted dynamic processes allow the exclusive detection of diffusion contribution from C2. Reprinted with permission from ref 292. Copyright 2000 Wiley VCH.

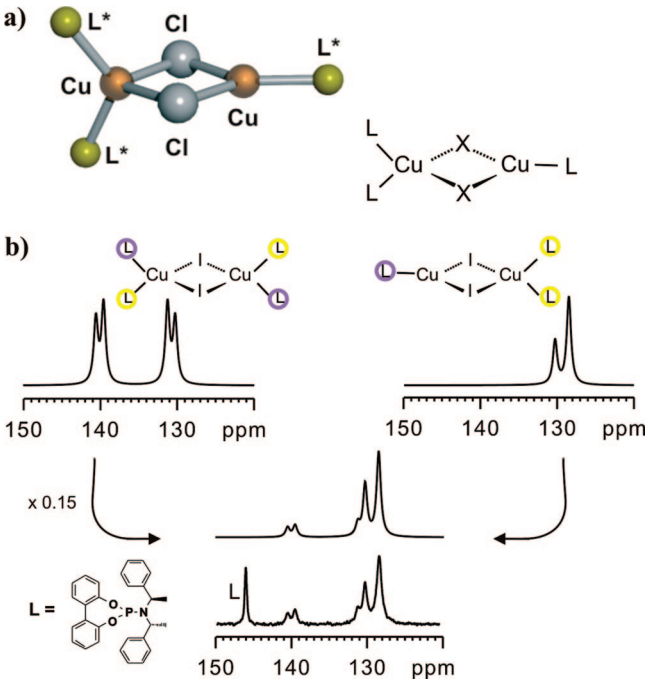

Figure 28. (a) Schematic representation of the precatalytic binuclear complex with mixed trigonal/tetrahedral coordination of copper. (Reprinted with permission from ref 292. Copyright 2000 Wiley VCH.) (b) Low temperature ^{31}P spectra of CuI and ligand **29** confirm the existence of these complex species at 172 K. In addition, small contributions of a binuclear complex with tetrahedral coordination on both copper atoms are detected.[302]

4.5. Diimine Copper Complexes

In a further noteworthy study, the precatalytic complex in copper mediated Ullmann and Goldberg reactions[309–311] is shown to exhibit an equilibrium between monomers and dimers in solution with the aid of a combined NMR, electrochemistry, and X-ray crystallography study[312] The configurational stability of copper (I) diimine complexes was studied in one case with EXSY spectra[313] and in another one with the aid of TRISPHAT anions (tris(tetrachlorobenzenediolato)phosphate(V)).[314] Naphthalene was found to bind to Cu(I) with a free energy around 12−13 kcal/mol for the barrier of the coordination/decoordination process in solution.[315]

In addition, a recent HRMAS NMR study on silica-immobilized Pd/Cu catalysts is notable, allowing an insight into the catalytically active species in Sonogashira reactions.[316] ^{31}P CP/MAS and HRMAS spectra show that the Sonogashira reaction does indeed take place on the surface with an intermediate Cu/Pd aggregate as active species, which is not persistent. The previously immobilized Pd complex acts as homogeneous component in the catalysis as it leaches during subsequent recycling steps.[316]

5. Conclusion

The reactivity and the high synthetic potential of copper complexes or metal organocuprate clusters is supposed to be based on their ability to form supramolecular structures. In an appropriate size, cooperative interactions within the polymetallic clusters are possible, which are able to tap the full potential of the Cu(I)/Cu(III) redox system. For a long time, the complexity in determining the structures of these aggregated species in solution, the existence of dynamic equilibria between several species, and the NMR spectroscopically unfavorable properties of the stable isotopes ^{63}Cu and ^{65}Cu hampered the structure elucidation of copper complexes in solution. One of the reasons is that in high resolution NMR it has not been possible until now to deal with the large quadrupole moments of ^{63}Cu and ^{65}Cu in a satisfactory manner. Therefore, ^{63}Cu and ^{65}Cu NMR spectroscopy is mainly applicable to complexes with rigorous tetrahedral coordination of copper. In such complexes with detectable and sharp ^{63}Cu and ^{65}Cu signals, for example, information about the π-acceptor properties of the copper bound ligands or ligand exchange contributions can be obtained. However, the synthetically important copper reagents, catalytic complexes, and intermediates exhibit in general no undisturbed tetrahedral coordination around the copper ion. Therefore, the NMR structural investigations of most of the copper compounds in solution are limited to the NMR active nuclei of ligands or substituents. Despite the

Scheme 7. Proposed Dissociation of the Binuclear Precatalytic Copper Complex with Ferrocene Derived Diphosphine Ligands upon Addition of Grignard Reagents[a]

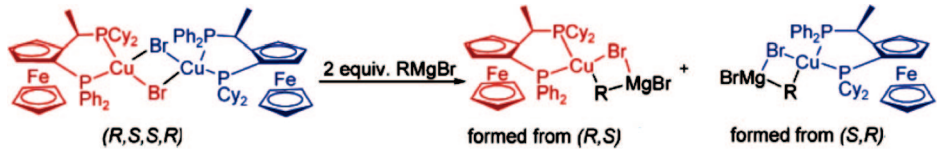

[a] Reprinted with permission from ref 306. Copyright 2006 American Chemical Society.

continually improving NMR methodology, the structure elucidation of such aggregated copper complexes in solution still remains a real challenge. This is mainly due to the fact that especially in highly symmetric aggregates with small ligands or substituents it is often not possible to apply the classical NMR spectroscopic approach for structure elucidation. But the application of diffusion NMR experiments allows the determination of the hydrodynamic radii of the aggregates and from sophisticated NOESY and HOESY experiments it is possible to gain insight into the structural details of these aggregates. Rapid-injection NMR and/or elaborated preparative stabilization methods combined with low temperature NMR enable the detection of decisive intermediate structures and often valuable scalar coupling information can be obtained with the aid of specific isotope labeling. In the past decade, specific combinations of these methods were especially used to elucidate the structure of dialkylcuprates and their intermediates in ethereal solutions. In diethyl ether, the oligomeric structure consists of homodimeric core units connected by salt- and solvent molecules with the supramolecular structure being decisive for the reactivity in 1,4-addition reactions to enones. Structural details about organocuprate π-complexes were obtained and even the elusive Cu(III) intermediates were stabilized for days and shown to be square planar. For amidocuprates, the dimer structure, its decomposition, and in one case structural isomers of amidocuprate dimers were reported. Also, the structure elucidation of precatalytic and catalytic copper complexes with chiral ligands made substantial progress. Especially in the case of copper complexes with TADDOL-like thiol ligands and with phosphoramidite ligands, detailed NMR spectroscopic studies revealed tetranuclear and binuclear copper complexes as precatalytic species. Thus, the recent progress in NMR structure elucidation of copper complexes allows a first glance on the fascinating supramolecular structures of copper compounds in solution, which are supposed to be crucial for the valuable reactivities and selectivities of copper reagents and catalysts.

6. Acknowledgments

I thank N. Kastner-Pustet for the processing of this manuscript and M. Schmid, R. Kleinmaier, T. Gärtner, and M. Rovira for language corrections.

7. References

(1) Feringa, B. L. *Acc. Chem. Res.* **2000**, *33*, 346–353.
(2) Lopez, F.; Minnaard, A. J.; Feringa, B. L. *Acc. Chem. Res.* **2007**, *40*, 179–188.
(3) Krause, N. *Modern Organocopper Chemistry*; Wiley-VCH: Weinheim, 2002.
(4) Dubbaka, S. R.; Kienle, M.; Mayr, H.; Knochel, P. *Angew. Chem., Int. Ed.* **2007**, *46*, 9093–9096.
(5) Knochel, P.; Yang, X.; Gommermann, N. *Handb. Funct. Organometallics* **2005**, *2*, 379–395.
(6) Palais, L.; Mikhel, I. S.; Bournaud, C.; Micouin, L.; Falciola, C. A.; Vuagnoux-d'Augustin, M.; Rosset, S.; Bernardinelli, G.; Alexakis, A. *Angew. Chem., Int. Ed.* **2007**, *46*, 7462–7465.
(7) Surry, D., S.; Spring, D. R. *Chem. Soc. Rev* **2006**, *35*, 218–225.
(8) Vuagnoux-d'Augustin, M.; Alexakis, A. *Eur. J. Org. Chem.* **2007**, 5852–5860.
(9) Baker, E. N. Copper Proteins with Type 1 Sites. In *Encyclopedia of Inorganic Chemistry*; King, R. B., Ed.; Wiley: New York, 1995; Vol. 2, p 883.
(10) Banci, L.; Pierattelli, R. Nuclear magnetic resonance spectroscopy studies on copper proteins. In *Advances in Protein Chemistry*, Vol. 60 (Copper-Containing Proteins); Academic Press: San Diego, CA, 2002; pp 397−449.
(11) McMillin, D. R.; Peyratout, C.; Miller, C. Copper Proteins: Oxidases. In *Encyclopedia of Inorganic Chemistry*; King, R. B., Ed.; Wiley: New York, 1995; Vol. 2, p 869.
(12) Nersissian, A. M.; Shipp, E. L. Blue copper-binding domains. In *Advances in Protein Chemistry*, Vol. 60 (Copper-Containing Proteins); Academic Press: San Diego, CA, 2002; p 271.
(13) Gaggelli, E.; Kozlowski, H.; Valensin, D.; Valensin, G. *Chem. Rev* **2006**, *106*, 1995–2044.
(14) Ford, P. C.; Fernandez, B. O.; Lim, M. D. *Chem. Rev.* **2005**, *105*, 2439–2455.
(15) Henkel, G.; Krebs, B. *Chem. Rev.* **2004**, *104*, 801–824.
(16) Kim, E.; Chufan, E. E.; Kamaraj, K.; Karlin, K. D. *Chem. Rev.* **2004**, *104*, 1077–1133.
(17) Solomon, E. I.; Szilagyi, R. K.; DeBeer, G. S.; Basumallick, L. *Chem. Rev.* **2004**, *104*, 419–458.
(18) Bertini, I.; Luchinat, C.; Parigi, G. *Prog. Magn. Reson. Spectrosc.* **2002**, *40*, 249–273.
(19) Bertini, I.; Luchinat, C.; Piccioli, M. *Prog. Magn. Reson. Spectrosc.* **1994**, *26*, 91–139.
(20) Kroneck, P.; Kodweiss, J.; Lutz, O.; Nolle, A.; Zepf, D. *Z. Naturforsch., Teil A.* **1982**, *37A*, 186–190.
(21) Wilkinson, G.; Gillard, R.; McCleverty, J. *Comprehensive Coordination Chemistry*, Vol. 5; Pergamon: New York, 1987.
(22) Nakamura, E.; Mori, S. *Angew. Chem., Int. Ed.* **2000**, *39*, 3750–3771.
(23) John, M.; Auel, C.; Behrens, C.; Marsch, M.; Harms, K.; Bosold, F.; Gschwind, R. M.; Rajamohanan, P. R.; Boche, G. *Chem.−Eur. J.* **2000**, *6*, 3060–3068.
(24) Xie, X.; Auel, C.; Henze, W.; Gschwind, R. M. *J. Am. Chem. Soc.* **2003**, *125*, 1595–1601.
(25) Nakamura, E.; Mori, S.; Morokuma, K. *J. Am. Chem. Soc.* **1997**, *119*, 4900–4910.
(26) Mori, S.; Nakamura, E. *Chem.−Eur. J.* **1999**, *5*, 1534–1543.
(27) Nakamura, E.; Yamanaka, M. *J. Am. Chem. Soc.* **1999**, *121*, 8941–8942.
(28) Nakamura, E.; Yoshikai, N. *Bull. Chem. Soc. Jpn.* **2004**, *77*, 1–12.
(29) Henze, W.; Vyater, A.; Krause, N.; Gschwind, R. M. *J. Am. Chem. Soc.* **2005**, *127*, 17335–17342.
(30) Macchioni, A.; Ciancaleoni, G.; Zuccaccia, C.; Zuccaccia, D. *Chem. Soc. Rev.* **2008**, *37*, 479–489, and references therein.
(31) Stilbs, P. *Prog. NMR Spectrosc.* **1987**, *19*, 1–45.
(32) Price, W. S. *Concepts Magn. Reson.* **1997**, *9*, 299–336.
(33) Price, W. S. *Concepts Magn. Reson.* **1998**, *10*, 197–237.
(34) Johnson, C. S. *Prog. Nucl. Magn. Reson.* **1999**, *34*, 203–256.
(35) Cohen, Y.; Avram, L.; Frish, L. *Angew. Chem., Int. Ed.* **2005**, *44*, 520–554.
(36) Dehner, A.; Kessler, H. *ChemBioChem* **2005**, *6*, 1550–1565.
(37) Pregosin, P. S. *Prog. Nucl. Magn. Reson. Spectrosc.* **2006**, *49*, 261–288, and references therein.
(38) Berners Price, S. J.; Ronconi, L.; Sadler, P. J. *Prog. Magn. Reson. Spectrosc.* **2006**, *49*, 65–98.
(39) Dybowski, C.; Neue, G. *Prog. Magn. Reson. Spectrosc.* **2002**, *41*, 153–170.
(40) Ernsting, J. M.; Gaemers, S.; Elsevier, C. J. *Magn. Reson. Chem.* **2004**, *42*, 721–736.
(41) Johnels, D.; Guenther, H. Solid state NMR spectroscopy. In *Organolithium Chemistry of Organolithium Compounds*; John Wiley & Sons: Chichester, U.K., 2004; pp137−203.
(42) Martins, J. C.; Biesemans, M.; Willem, R. *Prog. Magn. Reson. Spectrosc.* **2000**, *36*, 271–322.
(43) Penner, G. H.; Liu, X. *Prog. Magn. Reson. Spectrosc.* **2006**, *49*, 151–167.
(44) Priqueler, J. R. L.; Butler, I. S.; Rochon, F. D. *Appl. Spec. Rev.* **2006**, *41*, 185–226.
(45) Ramaprasad, S. *Prog. Magn. Reson. Spectrosc.* **2005**, *47*, 111–121.
(46) Still, B. M.; Kumar, P. G. A.; Aldrich-Wright, J. R.; Price, W. S. *Chem. Soc. Rev.* **2007**, *36*, 665–686.
(47) van der Klink, J. J.; Brom, H. B. *Prog. Magn. Reson. Spectrosc.* **2000**, *36*, 89–201.
(48) Wrackmeyer, B. *Mod. Magn. Reson.* **2006**, *1*, 457–459.
(49) Harris, R.; Becker, E.; Cabral De Menezes, S. M.; Goodfellow, R.; Granger, P. *Pure Appl. Chem.* **2001**, *73*, 1795–1818.
(50) Tang, J. A.; Ellis, B. D.; Warren, T. H.; Hanna, J. V.; Macdonald, C. L. B.; Schurko, R. W. *J. Am. Chem. Soc.* **2007**, *129*, 13049–13065.
(51) Marker, A.; Gunter, M. J. *J. Magn. Reson.* **1982**, *47*, 118–132.
(52) Mason, J. *Multinuclear NMR*; Plenum Press: New York, 1987; Chapter 21.
(53) Szymanska, I. *Pol. J. Chem.* **2006**, *80*, 1095–1117.
(54) Granger, P. *Transition Metal Nuclear Magnetic Resonace*; Elsevier: Amsterdam, 1991.
(55) Malito, J. *J. Annu. Rep. NMR Spectrosc.* **1999**, *38*, 265–287.

(56) Kroeker, S.; Wasylishen, R. E.; Hanna, J. V. *J. Am. Chem. Soc.* **1999**, *121*, 1582–1590.
(57) Bastow, T. J.; Whitfield, H. J. J. o. M. S. *J. Mol. Struct.* **1980**, *58*, 305–313.
(58) Okuda, T.; Hiura, M.; Yamada, K.; Negita, H. *Chem. Lett.* **1977**, *4*, 367–370.
(59) Ramaprabhu, S.; Amstutz, N.; Lucken, E. A. C. *Z. Naturforsch., A: Phys. Sci.* **1994**, *49*, 199–201.
(60) Ramaprabhu, S.; Lucken, E. A. C.; Bernardinelli, G. *J. Chem. Soc., Dalton Trans. Inorg. Chem* **1995**, *1*, 115–121.
(61) Lucken, E. A. C. *Z. Naturforsch., A: Phys. Sci.* **1994**, *49*, 155–166.
(62) Nakamura, Y.; Kumagai, K. *Phys. C* **1989**, *162−164*, 187–188.
(63) Itoh, M.; Karashima, K.; Kyogoku, M.; Aoki, I. *Physica C* **1989**, *160*, 177–184.
(64) Shimizu, T. *J. Phys. Soc. Jpn.* **1993**, *62*, 779–784.
(65) Shimizu, T.; Yasuoka, H.; Imai, T.; Tsuda, T.; Takabatake, T.; Nakazawa, Y.; Ishikawa, M. *J. Phys. Soc. Jpn.* **1988**, *57*, 2494–505.
(66) Young, B.-L.; Curro, N. J.; Sidorov, V. A.; Thompson, J. D.; Sarrao, J. L. *Phys. Rev. B* **2005**, *71*, 224106/1–224106/9.
(67) Walstedt, R. E.; Kojima, H.; Butch, N.; Bernhoeft, N. *Phys. Rev. Lett.* **2003**, *90*, 067601/1–067601/4.
(68) Carretta, P.; Sala, R.; Tedoldi, F.; Borsa, F.; Rigamonti, A. *Nuovo Cimento Soc. Ital. Fis. D* **1997**, *19D*, 1193–1198.
(69) Itoh, M.; Sugahara, M.; Yamauchi, T.; Ueda, Y. *Phys. Rev. B: Condens. Matter* **1996**, *54*, R9631–R9634.
(70) In high resolution NMR the ^{63}Cu nucleus is commonly used in experiments due to its higher receptivity, whereas ^{65}Cu is normally chosen for solid-state NMR experiments owing to its smaller quadrupole moment and higher γ.
(71) Geerts, R. L.; Huffman, J. C.; Folting, K.; Lemmen, T. H.; Caulton, K. G. *J. Am. Chem. Soc.* **1983**, *105*, 3503–3506.
(72) Szlyk, E.; Szymanska, I. *Polyhedron* **1999**, *18*, 2941–2948.
(73) Goodfellow, R. Post-Transition Metals, Copper to Mercury. In *Multinuclear NMR*; Mason J., Ed.; Plenum Press: New York, 1987.
(74) Lutz, O.; Oehler, H.; Kroneck, P. *Z. Physik A* **1978**, *288*, 17–21.
(75) Lutz, O.; Oehler, H.; Kroneck, P. *Z. Naturforsch.* **1978**, *33A*, 1021–1024.
(76) Kroneck, P.; Lutz, O.; Nolle, A.; Oehler, H. *Z. Naturforsch.* **1980**, *35A*, 221–225.
(77) Kitagawa, S.; Munakata, M.; Sasaki, M. *Inorg. Chem. Acta* **1986**, *120*, 77–80.
(78) Nilsson, K. B.; Persson, I. *J. Chem. Soc., Dalton Trans.* **2004**, *9*, 1312–1319.
(79) Fife, D. J.; Moore, W. M.; Morse, K. W. *Inorg. Chem.* **1984**, *23*, 1684–1691.
(80) Black, J. R.; Levason, W.; Spicer, M. D.; Webster, M. *J. Chem. Soc., Dalton Trans.* **1993**, *20*, 3129–3136.
(81) Doel, C. L.; Gibson, A. M.; Reid, G.; Frampton, C. *Polyhedron* **1995**, *14*, 3139–3146.
(82) Szlyk, E.; Kucharek, R.; Szymanska, I. *J. Coord. Chem.* **2001**, *53*, 55–67.
(83) Mohr, B.; Brooks, E. E.; Rath, N.; Deutsch, E. *Inorg. Chem.* **1991**, *30*, 4541–4545.
(84) Szlyk, E.; Kucharek, R.; Szymanska, I. *Pol. J. Chem.* **2001**, *75*, 337–344.
(85) Szlyk, E.; Kucharek, R.; Szymanska, I.; Pazderski, L. *Polyhedron* **2003**, *22*, 3389–3393.
(86) Berners Price, S. J.; Brevard, C.; Pagelot, A.; Sadler, P. J. *Inorg. Chem.* **1986**, *25*, 596–599.
(87) Kirillov, A. M.; Smolenski, P.; Guedes da Silva, M. F. C.; Pombeiro, A. J. L. *Eur. J. Inorg. Chem.* **2007**, *18*, 2686–2692.
(88) Irangu, J. K.; Jordan, R. B. *Inorg. Chem.* **2003**, *42*, 3934–3942.
(89) Ochsenbein, U.; Schlaepfer, C. W. *Helv. Chim. Acta* **1980**, *63*, 1926–1931.
(90) Endo, K.; Yamamoto, K.; Deguchi, K.; Matsushita, K. *Bull. Chem. Soc. Jpn.* **1987**, *60*, 2803–7.
(91) Connor, J. A.; Kennedy, R. J. *Polyhedron* **1988**, *7*, 161–162.
(92) Kitagawa, S.; Munakata, M. *Inorg. Chem.* **1984**, *23*, 4388–4390.
(93) Gill, D. S.; Byrne, L.; Quickenden, T. I. *Z. Naturforsch.* **1998**, *53a*, 1004–1008.
(94) Gill, D. S.; Kamp, U.; Doelle, A.; Zeidler, M. D. *Indian J. Chem.* **2001**, *40A*, 693–699.
(95) Gill, D. S.; Rodehüser, L.; Delpuech, J. J. *J. Chem. Soc., Faraday Trans.* **1990**, *86*, 2847–2852.
(96) Gill, D. S.; Rodehuser, L.; Rubini, P.; Delpuech, J. J. *J. Chem. Soc., Faraday Trans.* **1995**, *91*, 2307–2312.
(97) Gill, D. S.; Singh, J.; Singh, R.; Zamir, T.; Quickenden, T. I. *Indian J. Chem.* **1999**, *38A*, 913–920.
(98) Imai, S.; Fujisawa, K.; Kobayashi, T.; Shirasawa, N.; Fujii, H.; Yoshimura, T.; Kitajima, N.; Moro-oka, Y. *Inorg. Chem.* **1998**, *37*, 3066–3070.
(99) Black, J. R.; Champness, N. R.; Levason, W.; Reid, G. *Inorg. Chem.* **1996**, *35*, 1820–1824.
(100) Kujime, M.; Kurahashi, T.; Tomura, M.; Fujii, H. *Inorg. Chem.* **2007**, *46*, 541–551.
(101) Nakatsuji, H.; Kanda, K.; Endo, K. *J. Am. Chem. Soc.* **1984**, *106*, 4653–4660.
(102) Comba, P.; Katsichtis, C.; Nuber, B.; Pritzkow, H. *Eur. J. Inorg. Chem.* **1999**, 777–783.
(103) Lippard, S. J.; Mayerle, J. J. *Inorg. Chem.* **1972**, *11*, 753–759.
(104) Muetterties, E. L.; Alegranti, C. W. *J. Am. Chem. Soc.* **1970**, *92*, 4114–4115.
(105) Tolman, C. A. *Chem. Rev.* **1977**, *77*, 313–348.
(106) Cotton, F. A.; Wilkinson, G. *Advanced Inorganic Chemistry*; John Wiley & Sons: New York, 1988.
(107) Bowmaker, G. A.; Pabst, M.; Roesch, N.; Schmidbaur, H. *Inorg. Chem.* **1993**, *32*, 880–887.
(108) Bertz, S. H. *J. Am. Chem. Soc.* **1990**, *112*, 4031–4032.
(109) Lipshutz, B. H.; Sharma, S.; Ellsworth, E. L. *J. Am. Chem. Soc.* **1990**, *112*, 4032–4034.
(110) Bertz, S. H.; Nilsson, K.; Davidsson, Ö.; Snyder, J. P. *Angew. Chem., Int. Ed.* **1998**, *37*, 314–317.
(111) Gerold, A.; Jastrzebski, J. T. B. H.; Kronenburg, C. M. P.; Krause, N.; van Koten, G. *Angew. Chem., Int. Ed. Engl.* **1997**, *36*, 755–757.
(112) Gschwind, R. M.; Xie, X.; Rajamohanan, P. R.; Auel, C.; Boche, G. *J. Am. Chem. Soc.* **2001**, *123*, 7299–7304.
(113) Mobley, T. A.; Müller, F.; Berger, S. *J. Am. Chem. Soc.* **1998**, *120*, 1333–1334.
(114) Huang, H.; Liang, C. H.; Penner-Hahn, J. E. *Angew. Chem., Int. Ed.* **1998**, *37*, 1564–1566.
(115) Krause, N. *Angew. Chem., Int. Ed.* **1999**, *38*, 79–81.
(116) Nakamura, E.; Mori, S.; Morokuma, K. *J. Am. Chem. Soc.* **1998**, *120*, 8273–8274.
(117) Mori, S.; Nakamura, E. *Tetrahedron Lett.* **1999**, *40*, 5319–5322.
(118) Nakamura, E.; Yamanaka, M.; Mori, S. *J. Am. Chem. Soc.* **2000**, *122*, 1826–1827.
(119) Nakamura, E.; Y., M.; Y., N.; Mori, S. *Angew. Chem. Int. Ed* **2001**, *40*, 1935–1938.
(120) Kronenburg, C. M. P.; Jastrzebski, J. T. B. H.; Boersma, J.; Lutz, M.; Spek, A. L.; van Koten, G. *J. Am. Chem. Soc.* **2002**, *124*, 11675–11683.
(121) Bertz, S. H.; Carlin, C. M.; Deadwyler, D. A.; Murphy, M. D.; Ogle, C. A.; Seagle, P. *J. Am. Chem. Soc.* **2002**, *124*, 13650–13651.
(122) Lipshutz, B. H. In *Organometallics in Synthesis*; Schlosser, M., Ed.; Wiley: Chichester, U.K., 1994.
(123) *Organocopper Reagents: A practical approach*; Taylor, R. J. K., Ed.; Oxford University Press: Oxford, U.K., 1994.
(124) Krause, N. In *Metallorganische Chemie*; Spectrum Akademischer Verlag: Heidelberg, Germany, 1996; pp 175−191.
(125) Woodward, S. *Chem. Soc. Rev.* **2000**, *29*, 393–401.
(126) Krause, N.; Gerold, A. *Angew. Chem., Int. Ed. Engl.* **1997**, *36*, 186–204.
(127) Lipshutz, B. H.; James, B. *J. Org. Chem.* **1994**, *59*, 7585–7587.
(128) Lipshutz, B. H.; Wilhelm, R. S.; Floyd, D. M. *J. Am. Chem. Soc.* **1981**, *103*, 7672–7674.
(129) Lipshutz, B. H.; Wilhelm, R. S.; Kozlowski, J. A. *Tetrahedron* **1984**, *40*, 5005–5038.
(130) Hope, H.; Oram, D.; Power, P. P. *J. Am. Chem. Soc.* **1984**, *106*, 1149–1150.
(131) Hope, H.; Olmsted, M. M.; Power, P. P.; Sandell, J.; Xu, X. *J. Am. Chem. Soc.* **1985**, *107*, 4337–4338.
(132) Villacorta, G. M.; Pulla Rao, C.; Lippard, S. J. *J. Am. Chem. Soc.* **1988**, *110*, 3175–3182.
(133) Hwang, C.-S.; Power, P. P. *Organometallics* **1999**, *18*, 697–700.
(134) Kronenburg, C. M. P.; Jastrzebski, J. T. B. H.; Spek, A. L.; van Koten, G. *J. Am. Chem. Soc.* **1998**, *120*, 9688–9689.
(135) Boche, G.; Bosold, F.; Marsch, M.; Harms, K. *Angew. Chem., Int. Ed.* **1998**, *37*, 1684–1686.
(136) Davies, R. P.; Hornauer, S. *Eur. J. Inorg. Chem.* **2005**, 51–54.
(137) Mann, B. E. *Spectroscopic Properties of Inorganic and Organometallic Compounds* **2002**, *35*, 112–174.
(138) Bertz, S. H.; Nilsson, K.; Davidsson, O.; Snyder, J. P. *Angew. Chem.* **1998**, *110*, 327–331.
(139) Bertz, S. H. *J. Am. Chem. Soc.* **1991**, *113*, 5470–5471.
(140) Gschwind, R. M.; Rajamohanan, P. R.; John, M.; Boche, G. *Organometallics* **2000**, *19*, 2868–2873.
(141) Stemmler, T. L.; Barnhart, T. M.; Penner-Hahn, J. E.; Tucker, C. E.; Knochel, P.; Böhme, M.; Frenking, G. *J. Am. Chem. Soc.* **1995**, *117*, 12489–12497.
(142) van Koten, G.; Noltes, J. G. *J. Am. Chem. Soc.* **1979**, *101*, 6593–6599.
(143) Berg, D. J.; Boncella, J. M.; Andersen, R. A. *Organometallics* **2002**, *21*, 4622–4631.
(144) Eriksson, J.; Arvidsson, P. I.; Davidsson, O. *J. Am. Chem. Soc.* **2000**, *122*, 9310–9311.

(145) Kronenburg, C. M. P.; Jastrzebski, J. T. B. H.; Lutz, M.; Spek, A. L.; van Koten, G. *Organometallics* **2003**, *22*, 2312–2317.
(146) Fraenkel, G.; Fraenkel, A. M.; Geckle, M. J.; Schloss, F. *J. Am. Chem. Soc.* **1979**, *101*, 4745–4747.
(147) Seebach, D.; Haessig, R.; Gabriel, J. *Helv. Chim. Acta* **1983**, *66*, 308–337.
(148) Saspe, A.-M.; Schleyer, P. v. R. E. *Lithium Chemistry: A Theoretical and Experimental Overview*; Wiley: Chichester, 1995.
(149) Collum, D. B. *Acc. Chem. Res.* **1993**, *26*, 227–234.
(150) Corruble, A.; Davoust, D.; Desjardins, S.; Fressigne, C.; Giessner-Prettre, C.; Harrison-Marchand, A.; Houte, H.; Lasne, M.-C.; Maddaluno, J.; Oulyadi, H.; Valnot, J.-Y. *J. Am. Chem. Soc.* **2002**, *124*, 15267–15279.
(151) Gregory, K.; Schleyer, P. v. R.; Snaith, R. *Adv. Inorg. Chem.* **1991**, *37*, 47–142.
(152) Lucht, B. L.; Collum, D. B. *Acc. Chem. Res.* **1999**, *32*, 1035–1042.
(153) Mulvey, R. E. *Chem. Soc. Rev.* **1991**, *20*, 167–209.
(154) Sott, R.; Granander, J.; Hilmersson, G. *J. Am. Chem. Soc.* **2004**, *126*, 6798–6805.
(155) Olmstead, M. M.; Power, P. P. *Organometallics* **1990**, *9*, 1720–1722.
(156) Stemmler, T. L.; Penner-Hahn, J. E.; Knochel, P. *J. Am. Chem. Soc.* **1993**, *115*, 348–350.
(157) Barnhart, T. M.; Huang, H.; Snyder, J. P.; Penner-Hahn, J. E. *J. Org. Chem.* **1995**, *60*, 4310–4311.
(158) Snyder, J. P.; Bertz, S. H. *J. Org. Chem.* **1995**, *60*, 4312–4313.
(159) Snyder, J. P.; Spangler, D. P.; Behling, J. R.; Rossiter, B. E. *J. Org. Chem.* **1994**, *59*, 2665–2667.
(160) Bertz, S. H.; Miao, G.; Eriksson, M. M. *Chem. Commun.* **1996**, 815–816.
(161) Pearson, R. G.; Gergory, C. D. *J. Am. Chem. Soc.* **1976**, *98*, 4098–4104.
(162) Ashby, E. C.; Watkins, J. J. *J. Am. Chem. Soc.* **1977**, *99*, 5312–5317.
(163) Bertz, S. H.; Chopra, A.; Eriksson, M.; Ogle, C. A.; Seagle, P. *Chem.−Eur. J.* **1999**, *5*, 2680–2691.
(164) Ouannes, C.; Dressaire, G.; Langlois, Y. *Tetrahedron Lett.* **1977**, 815–818.
(165) Hallnemo, G.; Ullenius, C. *Tetrahedron* **1983**, *39*, 1621–1625.
(166) Bertz, S. H.; Dabbagh, G. *Tetrahedron* **1989**, *45*, 425–434.
(167) Whitesides, G. M.; Fischer, W. F., Jr.; San Filippo, J., Jr.; Bashe, R. W.; House, H. O. *J. Am. Chem. Soc.* **1969**, *91*, 4871–4882.
(168) Nakamura, E.; Mori, S.; Nakamura, M.; Morokuma, K. *J. Am. Chem. Soc.* **1997**, *119*, 4887–4899.
(169) Lipshutz, B. H.; Keith, J.; Buzard, D. J. *Organometallics* **1999**, *18*, 1571–1574.
(170) Eaborn, C.; Hitchcock, P. B.; Smith, J. D.; Sullivan, A. C. *J. Organomet. Chem.* **1984**, *263*, C23–C25.
(171) van Koten, G.; Jastrzebski, J. T. B. H.; Muller, F.; Stam, C. H. *J. Am. Chem. Soc.* **1985**, *107*, 697–698.
(172) Olmstead, M. M.; Power, P. P. *J. Am. Chem. Soc.* **1990**, *112*, 8008–8014.
(173) Lorenzen, N. P.; Weiss, E. *Angew. Chem.* **1990**, *102*, 322–324.
(174) Bertz, S. H.; Dabbagh, G.; He, X.; Power, P. P. *J. Am. Chem. Soc.* **1993**, *115*, 11640–11641.
(175) Liou, L. R.; McNeil, A. J.; Ramirez, A.; Toombes, G. E. S.; Gruver, J. M.; Collum, D. B. *J. Am. Chem. Soc.* **2008**, *130*, 4859–4868.
(176) Also see references in:(a) Kaufman, M. J.; Streitwieser, A., Jr *J. Am. Chem. Soc.* **1987**, *109*, 6092–6097.
(177) Collum, D. B.; Kahne, D.; Gut, S. A.; DePue, R. T.; Mohamadi, F.; Wanat, R. A.; Clardy, J.; Van Duyne, G. *J. Am. Chem. Soc.* **1984**, *106*, 4865–4869.
(178) Xu, F.; Reamer, R. A.; Tillyer, R.; Cummins, J. M.; Grabowski, E. J. J.; Reider, P. J.; Collum, D. B.; Huffman, J. C. *J. Am. Chem. Soc.* **2000**, *122*, 11212–11218.
(179) Bauer, W.; Clark, T.; Schleyer, P. v. R. *J. Am. Chem. Soc.* **1987**, *109*, 970–977.
(180) Bauer, W.; Müller, G.; Schleyer, P. v. R. *Angew. Chem., Int. Ed. Engl.* **1986**, *25*, 1103.
(181) Avent, A. G.; Eaborn, C.; El-Kehli, M. N. A.; Molla, M. E.; Smith, J. D.; Sullivan, A. C. *J. Am. Chem. Soc.* **1986**, *108*, 3854–3855.
(182) Günther, H.; Moskau, D.; Schmalz, D. *Angew. Chem.* **1987**, *99*, 1242–1250.
(183) Bauer, W.; Klusener, P. A. A.; Harder, S.; Kanters, J. A.; Duisenburg, A. J. M.; Brandsma, L.; Schleyer, P. v. R. *Organometallics* **1988**, *7*, 552–555.
(184) Bauer, W.; Schleyer, P. v. R. *Adv. Carbanion Chem.* **1992**, *1*, 89–175.
(185) Mo, H.; Pochapsky, T. C. *Prog. NMR Spectrosc.* **1997**, *30*, 1–38.
(186) Hilmersson, G.; Arvidsson, P. I.; Davidson, O.; Hakansson, M. *J. Am. Chem. Soc.* **1998**, *120*, 8143–8149.
(187) Brand, T.; Cabrita, E. J.; Berger, S. *Prog. Magn. Reson. Spectrosc.* **2005**, *46*, 159–196.
(188) Macchioni, A. *Chem. Rev* **2005**, *105*, 2039–2073.
(189) Pregosin, P. S.; Kumar, A. P. G.; Fernandez, I. *Chem. Rev.* **2005**, *105*, 2977–2998.
(190) Noggle, J. H.; Schirmer, R. E. *The Nuclear Overhauser Effekt: Chemical Applications*; Academic Press: New York, 1971.
(191) Köver, K. E.; Batta, G. *Prog. NMR Spectrosc.* **1987**, *19*, 223–266.
(192) Neuhaus, D.; Williamson, M. *The Nuclear Overhauser Effect in Structural and Conformational Analysis*; VCH: Weinheim, 1989.
(193) Bertz, S. H.; Eriksson, M.; Miao, G.; Snyder, J. P. *J. Am. Chem. Soc.* **1996**, *118*, 10906–10907.
(194) Böhme, M.; Frenking, G.; Reetz, M. T. *Organometallics* **1994**, *13*, 4237–4245.
(195) Bertz, S. H.; Vellekoop, A. S.; Smith, R. A. J.; Snyder, J. P. *Organometallics* **1995**, *14*, 1213–1220.
(196) Gregory, C. D.; Pearson, R. G. *J. Am. Chem. Soc.* **1976**, *98*, 4098–4104.
(197) Davies, R. P.; Hornauer, S.; White, A. J. P. *Chem. Comm.* **2007**, 304–306.
(198) Huang, H.; Alveraz, K.; Liu, Q.; Barnhart, T. M.; Snyder, J. P.; Penner-Hahn, J. E. *J. Am. Chem. Soc.* **1996**, *118*, 8808–8816, and 12252 (correction)
(199) Kronenburg, C. M. P.; Amijs, C. H. M.; Jastrzebski, J. T. B. H.; Lutz, M.; Spek, A. L.; van Koten, G. *Organometallics* **2002**, *21*, 4662–4671.
(200) Kawabata, J.; Fukushi, E.; J., M. *J. Am. Chem. Soc.* **1992**, *114*, 1115–1117.
(201) Wagner, R.; Berger, S. *Magn. Reson. Chem.* **1997**, *35*, 199–202.
(202) Gschwind, R. M.; Xie, X.; Rajamohanan, P. R. *Magn. Reson. Chem.* **2004**, *42*, 308–312, and references therein.
(203) Yang, J. K.; Cauble, D. F.; Berro, A. J.; Bauld, N. L.; Krische, M. *J. Org. Chem.* **2004**, *69*, 7979–7984.
(204) Haupts, U.; Maiti, S.; Schwille, P.; Webb, W. W. *Proc. Natl. Acad. Sci. U.S.A.* **1998**, *95*, 13573–13578.
(205) Su, Q.; Klinman, J. P. *Biochemistry* **1999**, *38*, 8572–8581.
(206) Murphy, M. D.; Ogle, C. A.; Bertz, S. H. *Chem. Commun.* **2005**, 854–856.
(207) McGarrity, J. F.; Ogle, C. A.; Brich, Z.; Loosli, H. R. *J. Am. Chem. Soc.* **1985**, *107*, 1810–1815.
(208) McGarrity, J. F.; Prodolliet, J. *J. Org. Chem.* **1984**, *49*, 4465–4470.
(209) Perrin, C. L.; Dwyer, T. J. *Chem. Rev.* **1990**, *90*, 935–967.
(210) Bain, A. D. *Prog. Magn. Reson. Spectrosc.* **2003**, *43*, 63–103.
(211) Pons, M.; Millet, O. *Prog. Magn. Reson. Spectrosc.* **2001**, *38*, 267–324.
(212) Jerschow, A.; Mueller, N. *J. Magn. Reson.* **1997**, *125*, 372–375.
(213) Sorland, G. H.; Seland, J. G.; Krane, J.; Anthonsen, H. W. *J. Magn. Reson.* **2000**, *142*, 323–325.
(214) Cabrita, E. J.; Berger, S. *Magn. Reson. Chem.* **2001**, *39*, S142–S148.
(215) Pochapsky, S. S.; Mo, H.; Pochapsky, T. C. *J. Chem. Soc., Chem. Commun.* **1995**, 2513–2514.
(216) Zuccaccia, D.; Macchioni, A. *Organometallics* **2005**, *24*, 3476–3486.
(217) Edward, J. T. *J. Chem. Educ.* **1970**, *47*, 261–270.
(218) Keresztes, I.; Williard, P. G. *J. Am. Chem. Soc.* **2000**, *122*, 10228–10229.
(219) Cabrita, E. J.; Berger, S.; Braeuer, P.; Kaerger, J. *J. Magn. Reson.* **2002**, *157*, 124–131.
(220) Bondi, A. *J. Phys. Chem.* **1964**, *68*, 441–451.
(221) Bloomfield, V. A. In *On-Line Biophysics Textbook*; Schuster, T. M., Ed.; Biophysical Society: Bethesda, MD, 2000; Vol. Separation and Hydrodynamics.
(222) Marcus, Y.; Hefter, G. *Chem. Rev.* **2004**, *104*, 3405–3452.
(223) Canisius, J.; Gerold, A.; Krause, N. *Angew. Chem., Int. Ed.* **1999**, *38*, 1644–1646.
(224) Bertz, S. H.; Smith, R. A. *J. Am. Chem. Soc.* **1989**, *111*, 8276–8277.
(225) Canisius, J.; Mobley, T. A.; Berger, S.; Krause, N. *Chem.−Eur. J.* **2001**, *7*, 2671–2675.
(226) Christenson, B.; Olsson, T.; Ullenius, C. *Tetrahedron* **1989**, *45*, 523–534.
(227) Hallnemo, G.; Olsson, T.; Ullenius, C. *J. Organomet. Chem.* **1985**, *282*, 133–144.
(228) Lindstedt, E. L.; Nilsson, M.; Olsson, T. *J. Organomet. Chem.* **1987**, *334*, 255–261.
(229) Nilsson, K.; Ullenius, C.; Krause, N. *J. Am. Chem. Soc.* **1996**, *118*, 4194–4195.
(230) Sharma, S.; Oehlschlager, A. C. *Tetrahedron* **1989**, *45*, 557–568.
(231) Ullenius, C.; Christenson, B. *Pure Appl. Chem.* **1988**, *60*, 57–64.
(232) Vellekoop, A. S.; Smith, R. A. J. *J. Am. Chem. Soc.* **1994**, *116*, 2902–2913.
(233) Krause, N. *J. Org. Chem.* **1992**, *57*, 3509–3512.
(234) Krause, N.; Wagner, R.; Gerold, A. *J. Am. Chem. Soc.* **1994**, *116*, 381–382.
(235) Eriksson, J.; Davidsson, O. *Organometallics* **2001**, *20*, 4763–4765.
(236) Bertz, S. H.; Cope, S.; Murphy, M.; Ogle, C. A.; Taylor, B. J. *J. Am. Chem. Soc.* **2007**, *129*, 7208–7209.

(237) Bartholomew, E. R.; Bertz, S. H.; Cope, S.; Dorton, D. C.; Murphy, M.; Ogle, C. A. *Chem. Comm.* **2008**, 1176–1177.
(238) Gaertner, T.; Henze, W.; Gschwind, R. M. *J. Am. Chem. Soc.* **2007**, *129*, 11362–11363.
(239) Yamanaka, M.; Nakamura, E. *Organometallics* **2001**, *20*, 5675–5681.
(240) Yamanaka, M.; Nakamura, E. *J. Am. Chem. Soc.* **2005**, *127*, 4697–4706.
(241) Mori, S.; Nakamura, E.; Morokuma, K. *Organometallics* **2004**, *23*, 1081–1088.
(242) Mori, S.; Uerdingen, M.; Krause, N.; Morokuma, K. *Angew. Chem., Int. Ed.* **2005**, *44*, 4715–4719.
(243) Yamanaka, M.; Kato, S.; Nakamura, E. *J. Am. Chem. Soc.* **2004**, *126*, 6287–6293.
(244) Norinder, J.; Baeckvall, J.-E.; Yoshikai, N.; Nakamura, E. *Organometallics* **2006**, *25*, 2129–2132.
(245) Yoshikai, N.; Yamashita, T.; Nakamura, E. *Angew. Chem., Int. Ed.* **2005**, *44*, 4721–4723.
(246) Snyder, J. P. *J. Am. Chem. Soc.* **1995**, *117*, 11025–11026.
(247) Uerdingen, M.; Krause, N. *Tetrahedron* **2000**, *56*, 2799–2804.
(248) Sharma, S.; Oehlschläger, A. C. *Tetrahedron* **1991**, *47*, 1177–1184.
(249) Bax, A.; Freeman, R.; Frenkiel, T. A. *J. Am. Chem. Soc.* **1981**, *103*, 2102–2104.
(250) Bax, A.; Mareci, T. H. *J. Magn. Reson.* **1983**, *53*, 360–363.
(251) Bodenhausen, G.; Kogler, H.; Ernst, R. R. *J. Magn. Reson.* **1984**, *58*, 370–388.
(252) Jin, L.; Kover, K. E.; Lenoir, M. R.; Uhrin, D. *J. Magn. Reson.* **2008**, *190*, 171–182.
(253) Keller, P. J.; Vogele, K. E. *J. Magn. Reson.* **1986**, *68*, 389–392.
(254) Sorensen, O. W.; Freeman, R.; Frenkiel, T.; Mareci, T. H.; Schuck, R. *J. Magn. Reson.* **1982**, *46*, 180–184.
(255) Sparks, S. W.; Ellis, P. D. *J. Magn. Reson.* **1985**, *62*, 1–11.
(256) Turner, D. L. *J. Magn. Reson.* **1982**, *49*, 175–178.
(257) (a) Henze, W.; Gärtner, T.; Gschwind, R. M. *J. Am. Chem. Soc.*, submitted. (b) Henze, W. PhD Thesis, Rheinische Friedrich-Wilhelms-Universität Bonn, 2005.
(258) Bertz, S. H.; Cope, S.; Dorton, D.; Murphy, M.; Ogle, C. A. *Angew. Chem., Int. Ed.* **2007**, *46*, 7082–7085.
(259) Bertz, S. H.; Dabbagh, G.; Mujsce, A. M. *J. Am. Chem. Soc.* **1991**, *113*, 631–636.
(260) House, H. O. *Acc. Chem. Res.* **1976**, *9*, 59–67.
(261) Hu, H.; Snyder, J. P. *J. Am. Chem. Soc.* **2007**, *129*, 7210–7211.
(262) Mori, S.; Nakamura, E.; Morokuma, K. *J. Am. Chem. Soc.* **2000**, *122*, 7294–7307.
(263) Mori, S.; Nakamura, E. In *Modern Organocopperchemistry*; Krause, N., Ed.; Wiley-VCH: Weinheim, 2001; pp 315−346 and references therein.
(264) Nakanishi, W.; Yamanaka, M.; Nakamura, E. *J. Am. Chem. Soc.* **2005**, *127*, 1446–1453.
(265) Nilsson, K.; Andersson, T.; Ullenius, C.; Gerold, A.; Krause, N. *Chem.−Eur. J.* **1998**, *4*, 2051–2058.
(266) Naumann, D.; Roy, T.; Tebbe, K. F.; Crump, W. *Angew. Chem., Int. Ed. Engl.* **1993**, *32*, 1482–1483.
(267) Willert-Porada, M. A.; Burton, D. J.; Baenziger, N. C. *J. Chem. Soc., Chem. Comm.* **1989**, 1633–1634.
(268) Melnik, M.; Kabesova, M. *J. Coord. Chem.* **2000**, *50*, 323–338.
(269) Frantz, D. E.; Singleton, D. A. *J. Am. Chem. Soc.* **2000**, *122*, 3288–3295.
(270) Frantz, D. E.; Singleton, D. A.; Snyder, J. P. *J. Am. Chem. Soc.* **1997**, *119*, 3383–3384.
(271) Nakano, K.; Bessho, Y.; Kitamura, M. *Chem. Lett.* **2003**, *32*, 224–225.
(272) Yoshikai, N.; Nakamura, E. *J. Am. Chem. Soc.* **2004**, *126*, 12264–12265.
(273) Singleton, D. A.; Thomas, A. A. *J. Am. Chem. Soc.* **1995**, *117*, 9357–9358.
(274) Dieter, R. K.; Hanks, T. W.; Lagu, B. *Organometallics* **1992**, *11*, 3549–3554.
(275) Dieter, R. K.; Tokles, M. *J. Am. Chem. Soc.* **1987**, *109*, 2040–2046.
(276) Rossiter, B. E.; Eguchi, M.; Miao, G.; Swingle, N. M.; Hernandez, A. E.; Vickers, D.; Fluckiger, E.; Patterson, R. G.; Reddy, K. V. *Tetrahedron* **1993**, *49*, 965–986.
(277) Armstrong, D. R.; Henderson, K. W.; Kennedy, A. R.; Kerr, W. J.; Mair, F. S.; Moir, J. H.; Moran, P. H.; Snaith, R. *J. Chem. Soc., Dalton Trans.* **1999**, 4063–4068.
(278) Aubrecht, K. B.; Lucht, B. L.; Collum, D. B. *Organometallics* **1999**, *18*, 2981–2987.
(279) Koizumi, T.; Morihashi, K.; Kikuchi, O. *Bull Soc. J.* **1996**, *69*, 305–309.
(280) Davies, R. P.; Hornauer, S.; Hitchcock, P. B. *Angew. Chem., Int. Ed.* **2007**, *46*, 5191–5194.
(281) Alam, T. M.; Pedrotty, D. M.; Boyle, T. J. *Magn. Reson. Chem.* **2002**, *40*, 361–365.
(282) Bauer, W. *Magn. Reson. Chem.* **1996**, *34*, 532–537.
(283) Bauer, W.; Schleyer, P. v. R. In *Lithium Chemistry: a Theoretical and Experimental Overview*; Wiley: New York, 1995; pp 125−172.
(284) Günther, H. In *Encyclopedia of Nuclear Magnetic Resonance*, Vol. 5; Grant, D. M., Harris, R. K., Eds.; Wiley: New York, 1996; pp 2807−2828.
(285) Pichota, A.; Pregosin, P. S.; Valentini, M.; Worle, M.; Seebach, D. *Angew. Chem., Int. Ed.* **2000**, *39*, 153–156.
(286) Seebach, D.; Jaeschke, G.; Pichota, A.; Audergon, L. *Helv. Chim. Acta* **1997**, *80*, 2515–2519.
(287) Girard, C.; Kagan, H. B. *Angew. Chem., Int. Ed.* **1998**, *37*, 2923–2959.
(288) Guillaneux, D.; Zhao, S.-H.; Samuel, O.; Rainford, D.; Kagan, H. B. *J. Am. Chem. Soc.* **1994**, *116*, 9430–9439.
(289) Reggelin, M. *Nachr. Chem. Tech. Lab.* **1997**, *45*, 392–396.
(290) Knotter, D. M.; Van Koten, G.; Van Maanen, H. L.; Grove, D. M.; Spek, A. L. *Angew. Chem.* **1989**, *101*, 351–352.
(291) Seebach, D.; Beck, A. K.; Heckel, A. *Angew. Chem., Int. Ed.* **2001**, *40*, 92–138.
(292) Zhang, H.; Gschwind, R. M. *Angew. Chem.* **2006**, *118*, 6540–6544.
(293) Alexakis, A.; Benhaim, C. *Eur. J. Org. Chem.* **2002**, 3221–3236.
(294) Alexakis, A.; Benhaim, C.; Rosset, S.; Humam, M. *J. Am. Chem. Soc.* **2002**, *124*, 5262–5263.
(295) Arnold, L. A.; Imbos, R.; Mandoli, A.; De Vries, A. H. M.; Naasz, R.; Feringa, B. L. *Tetrahedron* **2000**, *56*, 2865–2878.
(296) de Vries, A. H. M.; Meetsma, A.; Feringa, B. L. *Angew. Chem.* **1996**, *108*, 2526–2528.
(297) Shi, W.-J.; Wang, L.-X.; Fu, Y.; Zhu, S.-F.; Zhou, Q.-L. *Tetrahedron Asymmetry* **2003**, *14*, 3867–3872.
(298) Feringa, B. L.; Naasz, R.; Imbos, R.; Arnold, L. A. In *Modern Organocopper Chemistry*; Krause, N., Ed.; Wiley-VCH: Weinheim, 2002; pp 224−258.
(299) Dyason, J. C.; Engelhardt, L. M.; Pakawatchai, C.; Healy, P. C.; White, A. H. *Aust. J. Chem.* **1985**, *38*, 1243–1250.
(300) Gill, J. T.; Mayerle, J. J.; Welcker, P. S.; Lewis, D. F.; Ucko, D. A.; Barton, D. J.; Stowens, D.; Lippard, S. J. *Inorg. Chem.* **1976**, *15*, 1155–1168.
(301) Zhang, H.; Gschwind, R. M. *Chem.−Eur. J.* **2007**, *13*, 6691–6700.
(302) (a) Schober, K.; Zhang, H.; Gschwind, R. M. *J. Am. Chem. Soc.*, in press. (b) Zhang, H. PhD Thesis, Regensburg, 2007. (c) Schober, K. Diploma Thesis, Regensburg, 2007.
(303) Gallo, E.; Ragaini, F.; Bilello, L.; Cenini, S.; Gennari, C.; Piarulli, U. *J. Organomet. Chem.* **2004**, *689*, 2169–2176.
(304) Kitamura, M.; Miki, T.; Nakano, K.; Noyori, R. B. *Chem. Soc. Jpn.* **2000**, *73*, 999–1014.
(305) Pfretzschner, T.; Kleemann, L.; Janza, B.; Harms, K.; Schrader, T. *Chem.−Eur. J.* **2004**, *10*, 6048–6057.
(306) Harutyunyan, S. R.; Lopez, F.; Browne, W. R.; Correa, A.; Pena, D.; Badorrey, R.; Meetsma, A.; Minnaard, A.; Feringa, B. L. *J. Am. Chem. Soc.* **2006**, *128*, 9103–9118.
(307) Yan, M.; Yang, L.-W.; Wong, K.; Chan, A. S. C. *Chem. Comm.* **1999**, 11–12.
(308) Lopez, F.; Harutyunyan, S. R.; Meetsma, A.; Minnaard, A. J.; Feringa, B. L. *Angew. Chem., Int. Ed.* **2005**, *44*, 2752–2756.
(309) Kunz, K.; Scholz, U.; Ganzer, D. *Synlett* **2003**, 2428–2439.
(310) Ley, S. V.; Thomas, A. W. *Angew. Chem.* **2003**, *42*, 5400–5449.
(311) Monnier, F.; Taillefer, M. *Angew. Chem.* **2008**, *120*, 3140–3143.
(312) Ouali, A.; Taillefer, M.; Spindler, J.-F.; Jutand, A. *Organometallics* **2007**, *26*, 65–74.
(313) Pianet, I.; Vincent, J.-M. *Inorg. Chem.* **2004**, *43*, 2947–2953.
(314) Desvergnes-Breuil, V.; Hebbe, V.; Dietrich-Buchecker, C.; Sauvage, J.-P.; Lacour, J. *Inorg. Chem.* **2003**, *42*, 255–257.
(315) Conry, R. R.; Striejewske, W. S. *Organometallics* **1998**, *17*, 3146–3148.
(316) Posset, T.; Bluemel, J. *J. Am. Chem. Soc.* **2006**, *128*, 8394–8395.

CR800286R